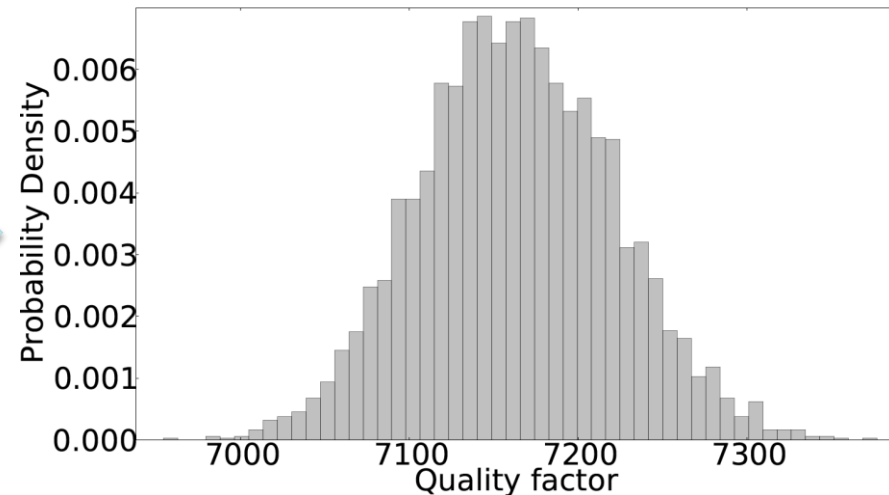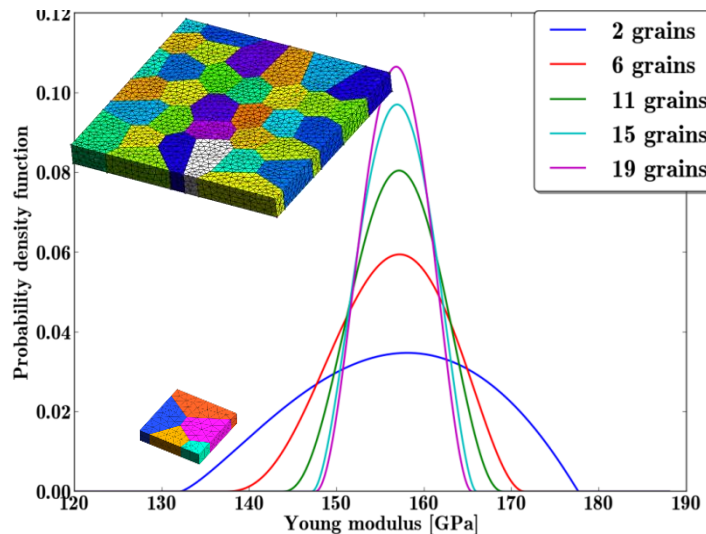# Probabilistic prediction of the quality factor of micro-resonator using a stochastic thermo-mechanical multi-scale approach

Wu Ling, Lucas Vincent, Nguyen Van-Dung, Paquay Stéphane,
Golinval Jean-Claude, Noels Ludovic
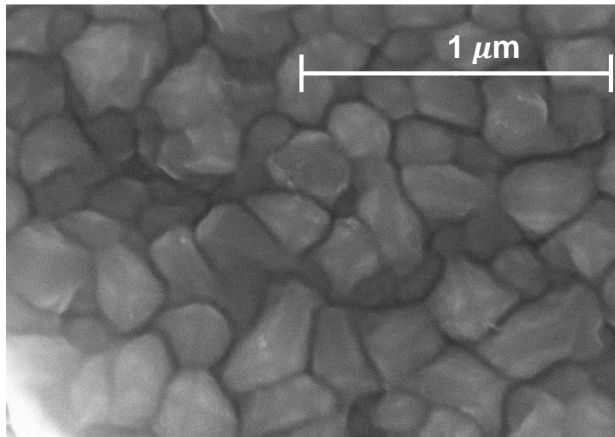*Voicu Rodica, Baracu Angela, Muller Raluca*

The problem

- ## MEMS structures
  - Are not several orders larger than their micro-structure size
  - Parameters-dependent manufacturing process
    - Low Pressure Chemical Vapor Deposition (LPCVD)
    - Properties depend on the temperature, time process, and flow gas conditions
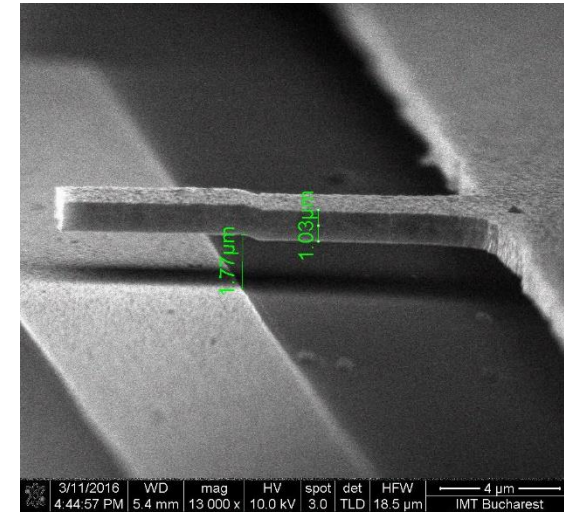
The problem

- Material structure: grain size distribution

    Measurement of SEM (Scanning electron microscope)

    – Grain size dependent on the LPCVD temperature process
    – 2 µm-thick poly-silicon films

Deposition temperature: 580 °C
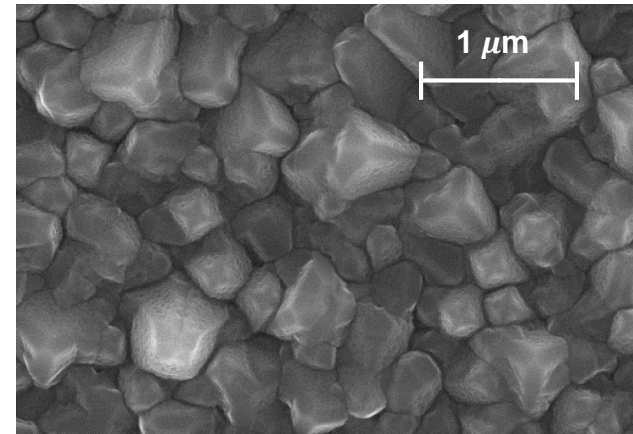
Deposition temperature: 650 °C

Temperature [°C]	580	610	630	650
Average grain diameter [µm]	0.21	0.45	0.72	0.83

SEM images provided by IMT Bucharest, Rodica Voicu, Angela Baracu, Raluca Muller

The problem

- Material structure: grain orientation distribution
  - Grain orientation by XRD (X-ray Diffraction) measurements on 2 μm-thick poly-silicon films
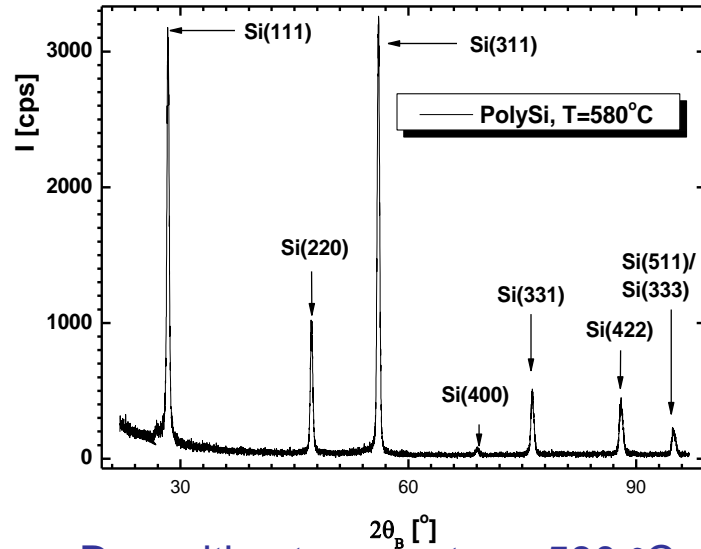
Deposition temperature: 580 °C
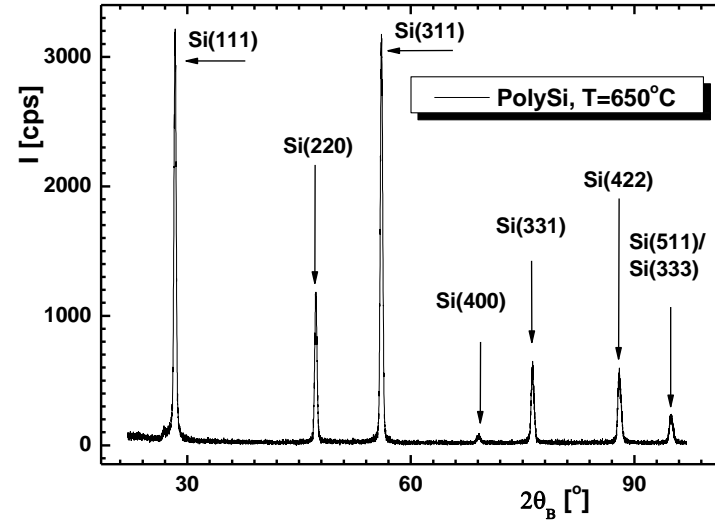
Deposition temperature: 630 °C

Temperature [°C]	580	610	630	650
<111> [%]	12.57	19.96	12.88	11.72
<220> [%]	7.19	13.67	7.96	7.59
<311> [%]	42.83	28.83	39.08	38.47
<400> [%]	4.28	5.54	3.13	3.93
<331> [%]	17.97	18.14	21.32	20.45
<422> [%]	15.15	13.86	15.63	17.84

XRD images provided by IMT Bucharest, Rodica Voicu, Angela Baracu, Raluca Muller

The problem

- ## Surface topology: asperity distribution

  - Upper surface topology by AFM (Atomic Force Microscope) measurements on 2 μm-thick poly-silicon films
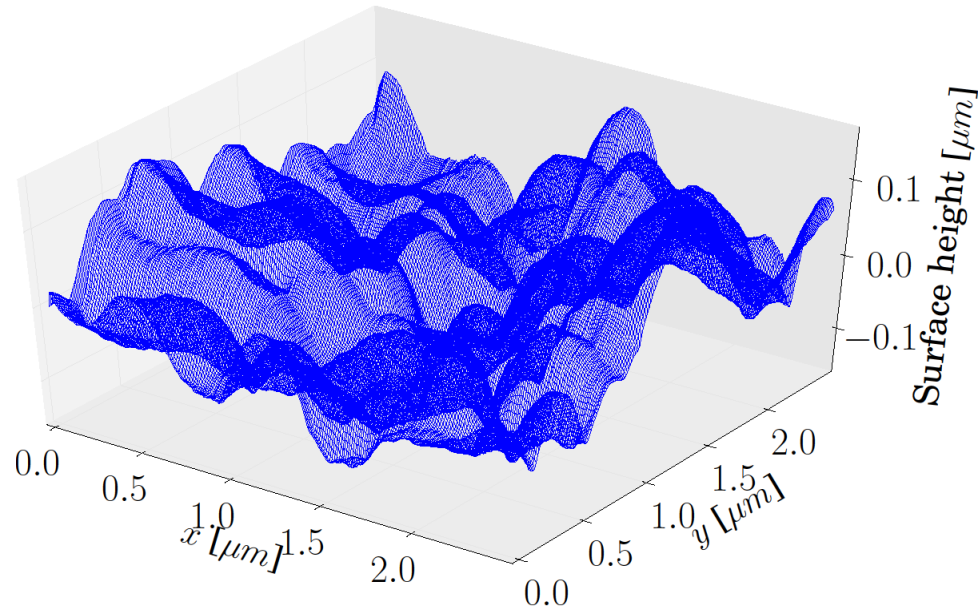
Temperature [°C]	580	610	630	650
Std deviation [nm]	35.6	60.3	90.7	88.3

AFM data provided by IMT Bucharest, Rodica Voicu, Angela Baracu, Raluca Muller

The problem

- **MEMS structures**
  - Are not several orders larger than their micro-structure size
  - Parameters-dependent manufacturing process
    - Low Pressure Chemical Vapor Deposition (LPCVD)
    - Properties depend on the temperature, time process, and flow gas conditions
  - As a result, their macroscopic properties can exhibit a **scatter**
    - Due to the fabrication process (photolithography, wet and dry etching)
    - Due to uncertainties of the material
    - …

  → The objective of this work is to estimate this scatter

- **Application example**
  - Poly-silicon resonators
  - Quantities of interest
    - Eigen frequency
    - Quality factor due to thermo-elastic damping
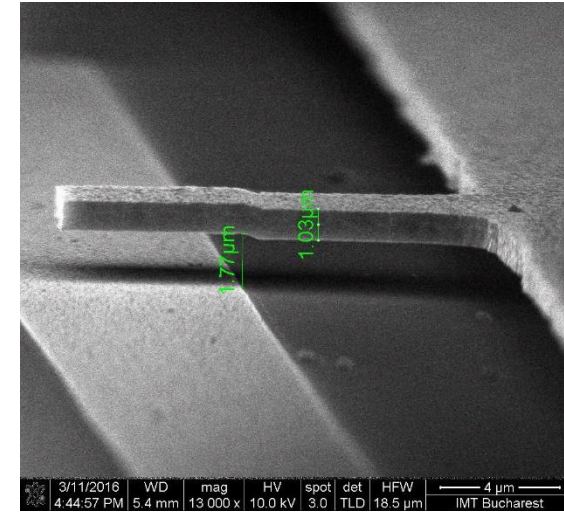
Monte-Carlo for a fully modelled beam

- The first mode frequency distribution can be obtained with
  - A 3D beam with each grain modelled
  - Grains according to experimental measurements
  - Monte-Carlo simulations
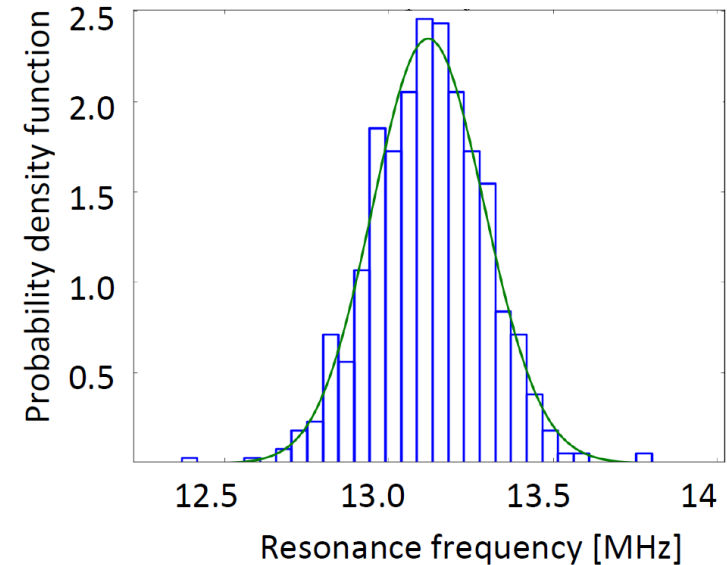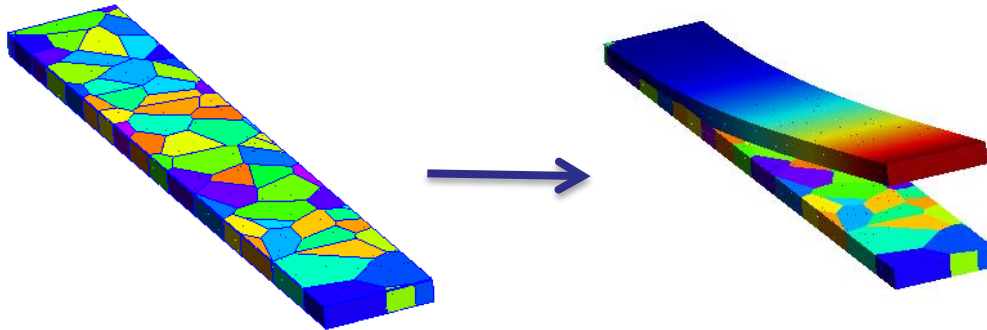
- Considering each grain is expensive and time consuming
  ↳ **Motivation for stochastic multi-scale methods**

Motivations

- ## Multi-scale modelling
  - 2 problems are solved concurrently
    - The macro-scale problem
    - The meso-scale problem (on a meso-scale Volume Element)

Material response

Extraction of a meso-scale Volume Element

Macro-scale

BVP
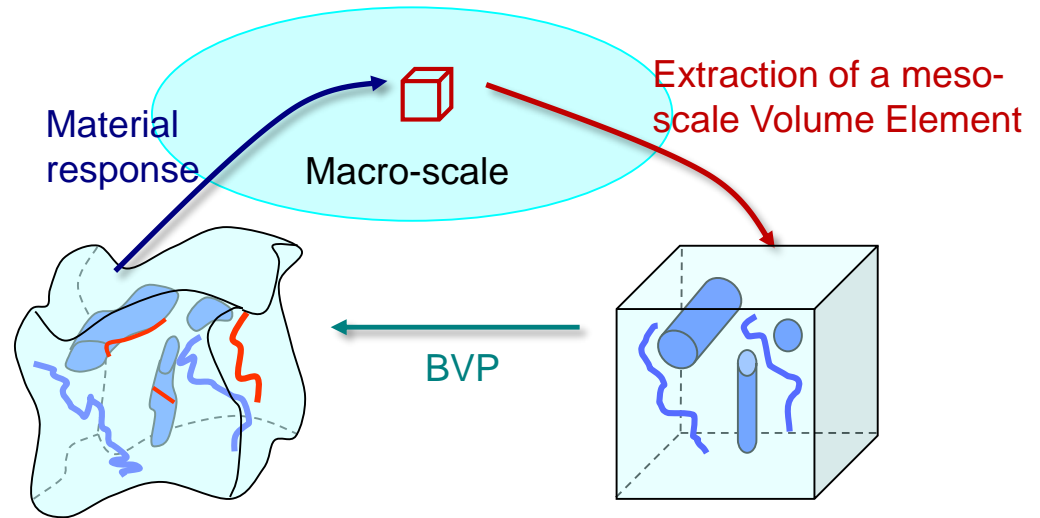
- ## Length-scales separation

$$L_{macro} >> L_{VE} >> L_{micro}$$

For accuracy: Size of the meso-scale volume element smaller than the characteristic length of the macro-scale loading

To be statistically representative: Size of the meso-scale volume element larger than the characteristic length of the micro-structure

Université de Liège

Motivations

- For structures not several orders larger than the micro-structure size

$$L_{\text{macro}} >> L_{\text{VE}} >\sim L_{\text{micro}}$$
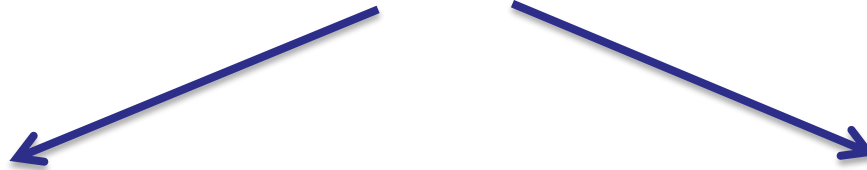
For accuracy: Size of the meso-scale volume element smaller than the characteristic length of the macro-scale loading

Meso-scale volume element no longer statistically representative: Stochastic Volume Elements*

- Possibility to propagate the uncertainties from the micro-scale to the macro-scale

*M Ostoja-Starzewski, X Wang, 1999
P Trovalusci, M Ostoja-Starzewski, M L De Bellis, A Murrali, 2015
X. Yin, W. Chen, A. To, C. McVeigh, 2008
J. Guilleminot, A. Noshadravan, C. Soize, R. Ghanem, 2011
….*

Université de Liège

A 3-scale process

Grain-scale or micro-scale	Meso-scale	Macro-scale
➢ Samples of the microstructure (volume elements) are generated ➢ Each grain has a random orientation	➢ Intermediate scale ➢ The distribution of the material property $\mathbb{P}(C)$ is defined	➢ Uncertainty quantification of the macro-scale quantity ➢ E.g. the first mode frequency $\mathbb{P}(f_1)$ /Quality factor $\mathbb{P}(Q)$
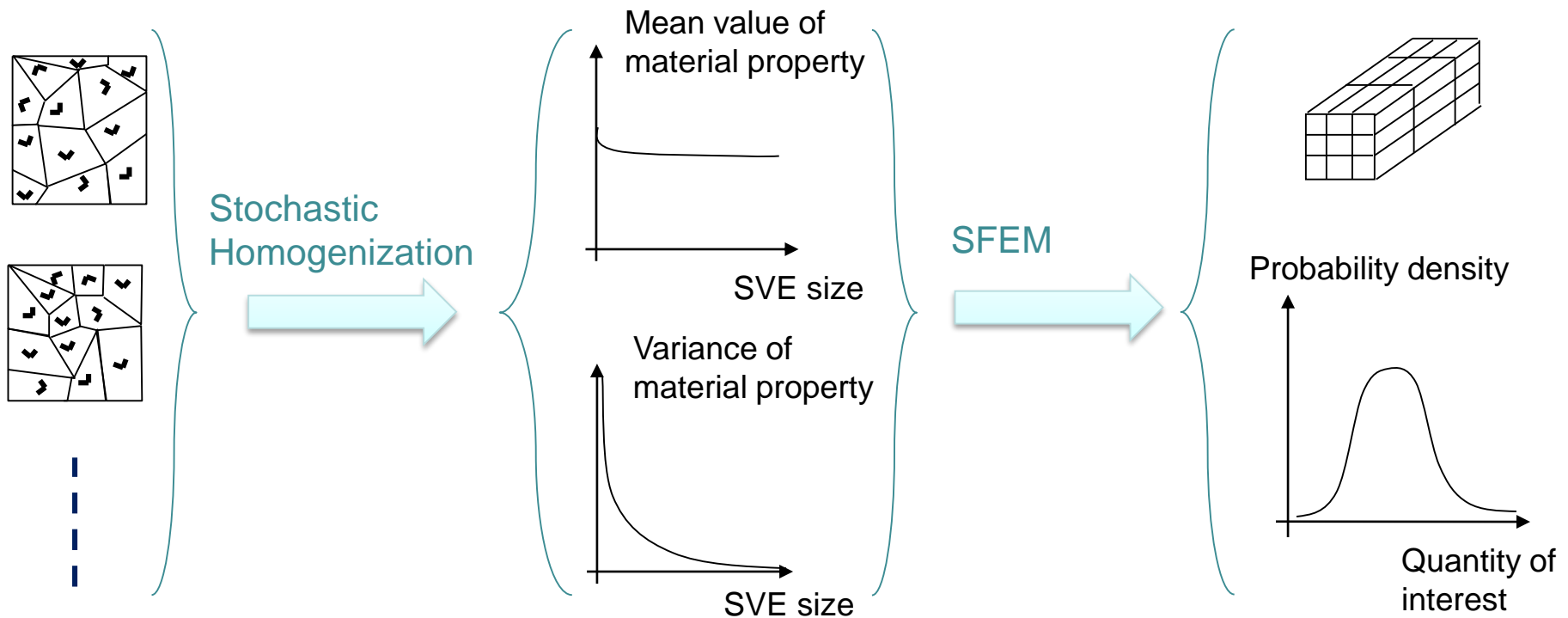
Stochastic Homogenization

Mean value of material property

SVE size

Variance of material property

SVE size

SFEM

Probability density

Quantity of interest

Université de Liège

- ## Thermo-mechanical problems
  - Governing equations
  - Macro-scale stochastic finite element
  - Meso-scale volume elements

$$\tau \ll T \quad \text{isothermal process}$$
$$\tau \gg T \quad \text{adiabatic process}$$
$$\tau \sim T \quad Q \downarrow$$

$$Q \sim \frac{W}{\Delta W}$$
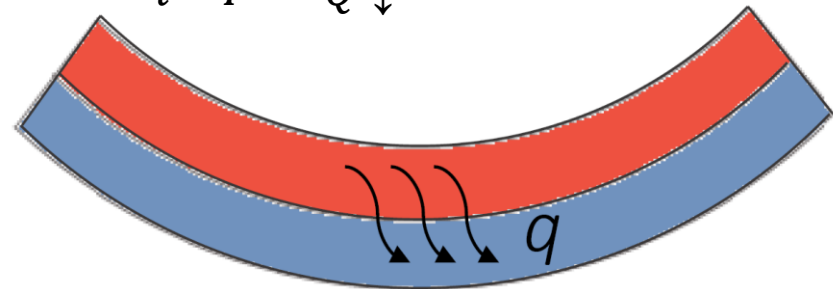
Thermoelastic damping is a source of intrinsic material <u>damping</u> due to thermoelasticity present in almost all materials

Content

- ## Thermo-mechanical problems
  – Governing equations
  – Macro-scale stochastic finite element
  – Meso-scale volume elements

- ## From the micro-scale to the meso-scale
  – Thermo-mechanical homogenization
  – Definition of Stochastic Volume Elements (SVEs) & Stochastic homogenization
  – Need for a meso-scale random field

- ## The meso-scale random field
  – Definition of the thermo-mechanical meso-scale random field
  – Stochastic model of the random field: Spectral generator & non-Gaussian mapping

- ## From the meso-scale to the macro-scale
  – 3-Scale approach verification
  – Application to extract the quality factor

- ## Extension to stochastic-plate finite elements
  – Second-order stochastic homogenization
  – Rough Stochastic Volume Elements
  – Topology uncertainties effects

Université de Liège

- ## Governing equations

  - ### Thermo-mechanics

    - **Linear balance** $\rho \ddot{\boldsymbol{u}} - \nabla \cdot \boldsymbol{\sigma} - \rho \boldsymbol{b} = 0$

    - **Clausius-Duhem inequality in terms of volume entropy rate** $\dot{S} = -\dfrac{\nabla \cdot \boldsymbol{q}}{T}$

    - **Helmholtz free energy**

$$
\begin{cases}
\mathcal{F}(\boldsymbol{\varepsilon}, T) = \mathcal{F}_0(T) - \boldsymbol{\varepsilon} : \dfrac{\partial^2 \psi}{\partial \boldsymbol{\varepsilon} \partial \boldsymbol{\varepsilon}} : \alpha(T - T_0) + \psi(\boldsymbol{\varepsilon}) \\[2em]
\boldsymbol{\sigma} = \left(\dfrac{\partial \mathcal{F}}{\partial \boldsymbol{\varepsilon}}\right)_T \quad , \quad S = \left(\dfrac{\partial \mathcal{F}}{\partial T}\right)_{\boldsymbol{\varepsilon}} \quad \& \quad \left(\dfrac{\partial^2 \mathcal{F}_0}{\partial T \partial T}\right) = \rho C_v
\end{cases}
$$

  - ### Strong form in terms of the displacements $\boldsymbol{u}$ and temperature change ϑ (linear elasticity)

$$
\begin{cases}
\rho \ddot{\boldsymbol{u}} - \nabla \cdot (\mathbb{C} : \dot{\boldsymbol{\varepsilon}} - \mathbb{C} : \boldsymbol{\alpha}\vartheta) - \rho \boldsymbol{b} = 0 \\[1.5em]
\rho C_v \dot{\vartheta} + T_0 \boldsymbol{\alpha} : \mathbb{C} : \dot{\boldsymbol{\varepsilon}} - \nabla \cdot (\boldsymbol{\kappa} \nabla \vartheta) = 0
\end{cases}
$$

  - ### Finite element discretization

$$
\begin{bmatrix} \mathbf{M}(\rho) & \mathbf{0} \\ \mathbf{0} & \mathbf{0} \end{bmatrix} \begin{bmatrix} \ddot{\mathbf{u}} \\ \ddot{\boldsymbol{\vartheta}} \end{bmatrix} + \begin{bmatrix} \mathbf{0} & \mathbf{0} \\ \mathbf{D}_{\vartheta u}(\boldsymbol{\alpha}, \mathbb{C}) & \mathbf{D}_{\vartheta\vartheta}(\rho C_v) \end{bmatrix} \begin{bmatrix} \dot{\mathbf{u}} \\ \dot{\boldsymbol{\vartheta}} \end{bmatrix} + \begin{bmatrix} \mathbf{K}_{uu}(\mathbb{C}) & \mathbf{K}_{u\vartheta}(\boldsymbol{\alpha}, \mathbb{C}) \\ \mathbf{0} & \mathbf{K}_{\vartheta\vartheta}(\boldsymbol{\kappa}) \end{bmatrix} \begin{bmatrix} \mathbf{u} \\ \boldsymbol{\vartheta} \end{bmatrix} = \begin{bmatrix} F_{\mathrm{u}} \\ F_{\vartheta} \end{bmatrix}
$$

Thermo-mechanical problem

- ## Macro-scale stochastic finite element method
  - Meso-scale material properties subjected to uncertainties
    - Elasticity tensor $\mathbb{C}_M(\boldsymbol{\theta})$,
    - Heat conductivity tensor $\boldsymbol{\kappa}_M(\boldsymbol{\theta})$, and
    - Thermal expansion tensors $\boldsymbol{\alpha}_M(\boldsymbol{\theta})$

    in the sample space $\boldsymbol{\theta} \in \boldsymbol{\Omega}$

$$\begin{bmatrix} \mathbf{M}(\rho_{\mathrm{M}}) & \mathbf{0} \\ \mathbf{0} & \mathbf{0} \end{bmatrix} \begin{bmatrix} \ddot{\mathbf{u}} \\ \ddot{\boldsymbol{\vartheta}} \end{bmatrix} + \begin{bmatrix} \mathbf{0} & \mathbf{0} \\ \mathbf{D}_{\vartheta\mathrm{u}}(\boldsymbol{\alpha}_{\mathrm{M}}, \mathbb{C}_{\mathrm{M}}) & \mathbf{D}_{\vartheta\vartheta}(\rho_{\mathrm{M}} C_{v\mathrm{M}}) \end{bmatrix} \begin{bmatrix} \dot{\mathbf{u}} \\ \dot{\boldsymbol{\vartheta}} \end{bmatrix} + \begin{bmatrix} \mathbf{K}_{\mathrm{uu}}(\mathbb{C}_{\mathrm{M}}) & \mathbf{K}_{\mathrm{u}\vartheta}(\boldsymbol{\alpha}_{\mathrm{M}}, \mathbb{C}_{\mathrm{M}}) \\ \mathbf{0} & \mathbf{K}_{\vartheta\vartheta}(\boldsymbol{\kappa}_{\mathrm{M}}) \end{bmatrix} \begin{bmatrix} \mathbf{u} \\ \boldsymbol{\vartheta} \end{bmatrix} = \begin{bmatrix} \boldsymbol{F}_{\mathrm{u}} \\ \boldsymbol{F}_{\vartheta} \end{bmatrix}$$

$$\longrightarrow \begin{bmatrix} \mathbf{M} & \mathbf{0} \\ \mathbf{0} & \mathbf{0} \end{bmatrix} \begin{bmatrix} \ddot{\mathbf{u}} \\ \ddot{\boldsymbol{\vartheta}} \end{bmatrix} + \begin{bmatrix} \mathbf{0} & \mathbf{0} \\ \mathbf{D}_{\vartheta\mathrm{u}}(\boldsymbol{\theta}) & \mathbf{D}_{\vartheta\vartheta} \end{bmatrix} \begin{bmatrix} \dot{\mathbf{u}} \\ \dot{\boldsymbol{\vartheta}} \end{bmatrix} + \begin{bmatrix} \mathbf{K}_{\mathrm{uu}}(\boldsymbol{\theta}) & \mathbf{K}_{\mathrm{u}\vartheta}(\boldsymbol{\theta}) \\ \mathbf{0} & \mathbf{K}_{\vartheta\vartheta}(\boldsymbol{\theta}) \end{bmatrix} \begin{bmatrix} \mathbf{u} \\ \boldsymbol{\vartheta} \end{bmatrix} = \begin{bmatrix} \boldsymbol{F}_{\mathrm{u}} \\ \boldsymbol{F}_{\vartheta} \end{bmatrix}$$

- ## Defining the random properties at the meso-scale by
  - Using micro-scale information (SEM, XRD, images)
  - Homogenization method

Université de Liège

Content

Thermo-mechanical problem

- **Meso-scale Volume Elements (VE)**
  - Micro-scale material properties
    - Elasticity tensor $\mathbb{C}_m$,
    - Heat conductivity tensor $\boldsymbol{\kappa}_m$, and
    - Thermal expansion tensors $\boldsymbol{\alpha}_m$

    defined on each phase/heterogeneity

$\mathbb{C}_{\mathrm{m}^i}, \kappa_{\mathrm{m}^i}, \alpha_{\mathrm{m}^i}$ $\mathbb{C}_{\mathrm{m}^i}, \kappa_{\mathrm{m}^i}, \alpha_{\mathrm{m}^i}$ $\mathbb{C}_{\mathrm{m}^i}, \kappa_{\mathrm{m}^i}, \alpha_{\mathrm{m}^i}$ $\mathbb{C}_{\mathrm{m}^i}, \kappa_{\mathrm{m}^i}, \alpha_{\mathrm{m}^i}$ $\mathbb{C}_{\mathrm{m}^i}, \kappa_{\mathrm{m}^i}, \alpha_{\mathrm{m}^i}$

  - Length scales separation assumptions
    - VE small enough for the time for strain wave to propagate in the SVE to remain negligible
    - VE small enough for the time variation of heat storage to remain negligible

$$\begin{bmatrix} \mathbf{M}(\rho_{\mathrm{m}}) & \mathbf{0} \\ \mathbf{0} & \mathbf{0} \end{bmatrix}\begin{bmatrix} \ddot{\mathbf{u}} \\ \ddot{\boldsymbol{\vartheta}} \end{bmatrix} + \begin{bmatrix} \mathbf{0} & \mathbf{0} \\ \mathbf{D}_{\vartheta\mathrm{u}}(\boldsymbol{\alpha}_{\mathrm{m}}, \mathbb{C}_{\mathrm{m}}) & \mathbf{D}_{\vartheta\vartheta}(\rho_{\mathrm{m}} C_{v\mathrm{m}}) \end{bmatrix}\begin{bmatrix} \dot{\mathbf{u}} \\ \dot{\boldsymbol{\vartheta}} \end{bmatrix} + \begin{bmatrix} \mathbf{K}_{\mathrm{uu}}(\mathbb{C}_{\mathrm{m}}) & \mathbf{K}_{\mathrm{u}\vartheta}(\boldsymbol{\alpha}_{\mathrm{m}}, \mathbb{C}_{\mathrm{m}}) \\ \mathbf{0} & \mathbf{K}_{\vartheta\vartheta}(\boldsymbol{\kappa}_{\mathrm{m}}) \end{bmatrix}\begin{bmatrix} \mathbf{u} \\ \boldsymbol{\vartheta} \end{bmatrix} = \begin{bmatrix} \boldsymbol{F}_{\mathrm{u}} \\ \boldsymbol{F}_{\vartheta} \end{bmatrix}$$

$$\begin{bmatrix} \mathbf{K}_{\mathrm{uu}} & \mathbf{K}_{\mathrm{u}\vartheta} \\ \mathbf{0} & \mathbf{K}_{\vartheta\vartheta} \end{bmatrix}\begin{bmatrix} \mathbf{u} \\ \boldsymbol{\vartheta} \end{bmatrix} = \begin{bmatrix} \boldsymbol{F}_{\mathrm{u}} \\ \boldsymbol{F}_{\vartheta} \end{bmatrix}$$

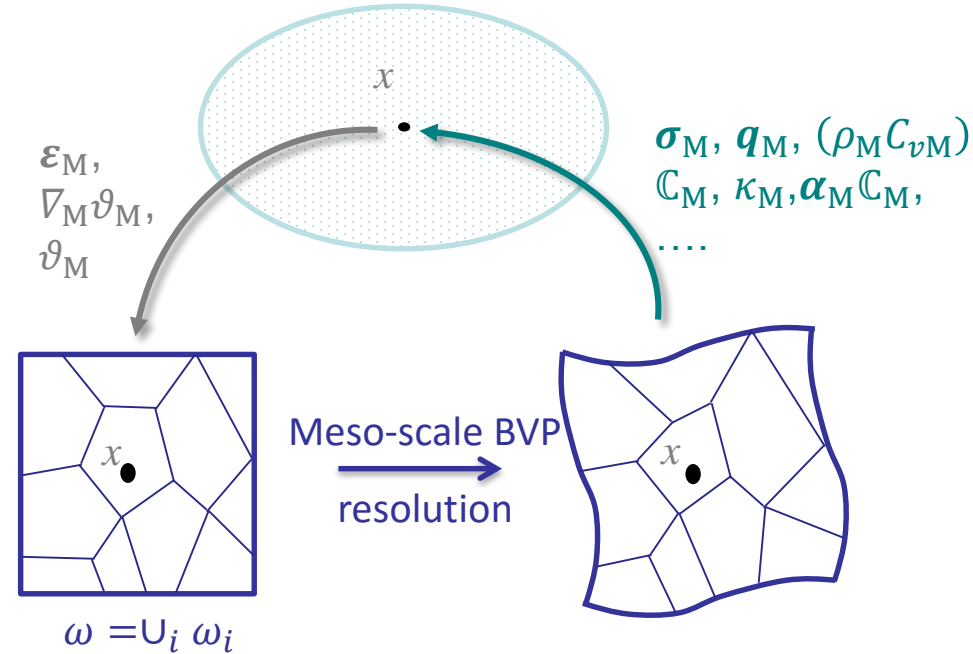- **Transition from meso-scale BVP realizations to the meso-scale random properties**

  Stochastic thermo-mechanical homogenization

From the micro-scale to the meso-scale

- **Thermo-mechanical homogenization**

  – Down-scaling

$$\begin{cases} \boldsymbol{\varepsilon}_M = \dfrac{1}{V(\omega)} \displaystyle\int_\omega \boldsymbol{\varepsilon}_m \, d\omega \\[2mm] \nabla_M \vartheta_M = \dfrac{1}{V(\omega)} \displaystyle\int_\omega \nabla_m \vartheta_m \, d\omega \\[2mm] \vartheta_M = \dfrac{1}{V(\omega)} \displaystyle\int_\omega \dfrac{\rho_m C_{vm}}{\rho_M C_{vM}} \vartheta_m \, d\omega \end{cases}$$

$\boldsymbol{\varepsilon}_M,$
$\nabla_M \vartheta_M,$
ϑ_M

x

$\boldsymbol{\sigma}_M, \boldsymbol{q}_M, (\rho_M C_{vM})$
$\mathbb{C}_M, \kappa_M, \boldsymbol{\alpha}_M \mathbb{C}_M,$
....

x

Meso-scale BVP
resolution

x

$\omega = \cup_i \omega_i$

  – Meso-scale BVP fluctuation fields

$$\llcorner\!\!\rightarrow \begin{cases} \boldsymbol{u}_m = \boldsymbol{\varepsilon}_M \cdot \boldsymbol{x} + \boldsymbol{u}' \\[2mm] \vartheta_m = \nabla_M \vartheta_M \cdot \boldsymbol{x} + \vartheta'_m \end{cases} \quad \longrightarrow \quad \begin{cases} 0 = \displaystyle\int_{\partial\omega} \boldsymbol{u}' \otimes \boldsymbol{n} \, d\partial\omega \\[2mm] 0 = \displaystyle\int_{\partial\omega} \boldsymbol{n} \vartheta' \, d\partial\omega \end{cases}$$

Satisfied by periodic boundary conditions

From the micro-scale to the meso-scale

- Thermo-mechanical homogenization (2)
  - Upscaling

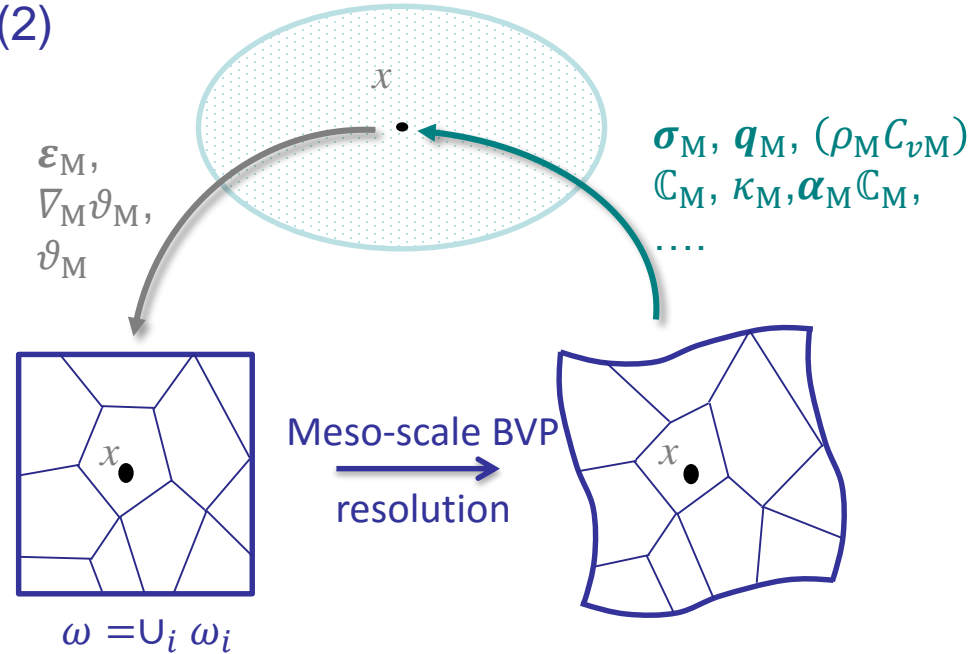$$\left\{ \begin{array}{l} \boldsymbol{\sigma}_{\mathrm{M}} = \dfrac{1}{V(\omega)} \int_{\omega} \boldsymbol{\sigma}_{\mathrm{m}} \, d\omega \\[12pt] \boldsymbol{q}_{\mathrm{M}} = \dfrac{1}{V(\omega)} \int_{\omega} \boldsymbol{q}_{\mathrm{m}} \, d\omega \\[12pt] \rho_{\mathrm{M}} C_{v\mathrm{M}} = \dfrac{1}{V(\omega)} \int \rho_{\mathrm{m}} C_{vm} \, dV \end{array} \right.$$

x

$\boldsymbol{\varepsilon}_{\mathrm{M}}, \\ \nabla_{\mathrm{M}} \vartheta_{\mathrm{M}}, \\ \vartheta_{\mathrm{M}}$

$\boldsymbol{\sigma}_{\mathrm{M}}, \boldsymbol{q}_{\mathrm{M}}, (\rho_{\mathrm{M}} C_{v\mathrm{M}})$ \
$\mathbb{C}_{\mathrm{M}}, \kappa_{\mathrm{M}}, \boldsymbol{\alpha}_{\mathrm{M}} \mathbb{C}_{\mathrm{M}},$ \
....

x

Meso-scale BVP resolution

x

$\omega = \cup_i \omega_i$

  - Consistency

$$\left\{ \begin{array}{l} \boldsymbol{\sigma}_{\mathrm{M}} : \delta \boldsymbol{\varepsilon}_{\mathrm{M}} = \dfrac{1}{V(\omega)} \int_{\omega} \boldsymbol{\sigma}_{\mathrm{m}} : \delta \boldsymbol{\varepsilon}_{\mathrm{m}} \, d\omega \\[12pt] \dfrac{\boldsymbol{q}_{\mathrm{M}} \cdot \nabla_{\mathrm{M}} \delta \vartheta_{\mathrm{M}}}{T_{\mathrm{M}}} \simeq \dfrac{1}{T_{\mathrm{M}} V(\omega)} \int_{\omega} \boldsymbol{q}_{\mathrm{m}} \cdot \nabla_{\mathrm{m}} \delta \vartheta_{\mathrm{m}} \, d\omega \\[12pt] \rho_{\mathrm{M}} C_{v\mathrm{M}} \vartheta_{\mathrm{M}} = \dfrac{1}{V(\omega)} \int_{\omega} \rho_{\mathrm{m}} C_{vm} \vartheta_{\mathrm{m}} \, d\omega \end{array} \right.$$

$$\left\{ \begin{array}{l} 0 = \int_{\partial\omega} (\boldsymbol{\sigma}_{\mathrm{m}} \cdot \boldsymbol{n}) \cdot \boldsymbol{u}' \, d\partial\omega \\[12pt] 0 = \int_{\partial\omega} (\boldsymbol{q}_{\mathrm{m}} \cdot \boldsymbol{n}) \vartheta' \, d\partial\omega \\[12pt] \vartheta_{\mathrm{M}} = \dfrac{1}{V(\omega)} \int_{\omega} \dfrac{\rho_{\mathrm{m}} C_{vm}}{\rho_{\mathrm{M}} C_{v\mathrm{M}}} \vartheta_{\mathrm{m}} \, d\omega \end{array} \right.$$

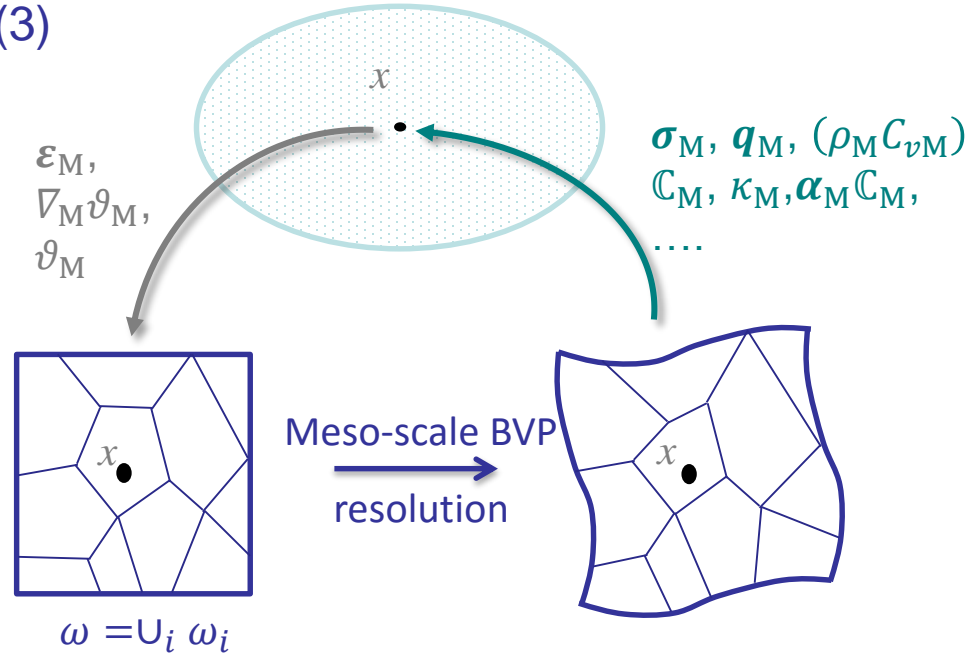Satisfied by periodic boundary conditions & volume constraint

From the micro-scale to the meso-scale

- Thermo-mechanical homogenization (3)
  - Micro-scale BVP

$$
\begin{cases}
\begin{bmatrix} \mathbf{K}_{uu} & \mathbf{K}_{u\vartheta} \\ \mathbf{0} & \mathbf{K}_{\vartheta\vartheta} \end{bmatrix} \begin{bmatrix} \mathbf{u} \\ \boldsymbol{\vartheta} \end{bmatrix} = \begin{bmatrix} \boldsymbol{F}_u \\ \boldsymbol{F}_\vartheta \end{bmatrix} \\[2em]
\mathbf{C} \begin{bmatrix} \mathbf{u} \\ \boldsymbol{\vartheta} \end{bmatrix} = \mathbf{S} \begin{bmatrix} \nabla_M \boldsymbol{u}_M \\ \nabla_M \vartheta_M \\ \vartheta_M \end{bmatrix}
\end{cases}
$$

x

$\boldsymbol{\varepsilon}_M,$
$\nabla_M \vartheta_M,$
ϑ_M

$\boldsymbol{\sigma}_M, \boldsymbol{q}_M, (\rho_M C_{vM})$
$\mathbb{C}_M, \kappa_M, \boldsymbol{\alpha}_M \mathbb{C}_M,$
....

Meso-scale BVP resolution

x

x

$\omega = \cup_i \omega_i$

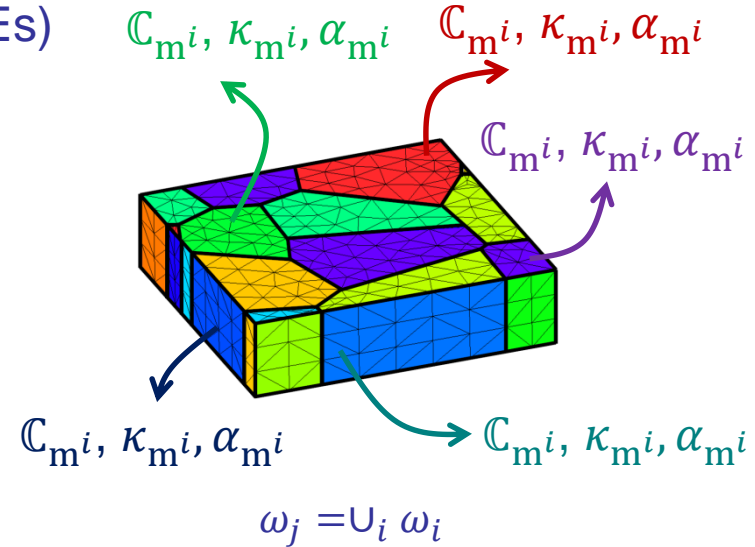- Solution is the stationary point of

$$
\Psi = \begin{bmatrix} \mathbf{u} \\ \boldsymbol{\vartheta} \end{bmatrix}^T \begin{bmatrix} \mathbf{K}_{uu} & \mathbf{K}_{u\vartheta} \\ \mathbf{0} & \mathbf{K}_{\vartheta\vartheta} \end{bmatrix} \begin{bmatrix} \mathbf{u} \\ \boldsymbol{\vartheta} \end{bmatrix} - \boldsymbol{\lambda}^T \begin{bmatrix} \mathbf{C} \begin{bmatrix} \mathbf{u} \\ \boldsymbol{\vartheta} \end{bmatrix} - \mathbf{S} \begin{bmatrix} \nabla_M \boldsymbol{u}_M \\ \nabla_M \vartheta_M \\ \vartheta_M \end{bmatrix} \end{bmatrix}
$$

$$
\begin{cases}
\boldsymbol{\sigma}_M = \dfrac{1}{V(\omega)} \dfrac{\partial \Psi}{\partial \boldsymbol{u}_M \otimes \boldsymbol{\nabla}_M} \\[1.5em]
\boldsymbol{q}_M = \dfrac{1}{V(\omega)} \dfrac{\partial \Psi}{\partial \nabla_M \vartheta_M}
\end{cases}
$$

$$
\begin{cases}
\mathbb{C}_M = \dfrac{\partial \boldsymbol{\sigma}_M}{\partial \boldsymbol{u}_M \otimes \boldsymbol{\nabla}_M} \quad \& \quad \boldsymbol{\alpha}_M : \mathbb{C}_M = -\dfrac{\partial \boldsymbol{\sigma}_M}{\partial \vartheta_M} \\[1.5em]
\kappa_M = -\dfrac{\partial \boldsymbol{q}_M}{\partial \nabla_M \vartheta_M}
\end{cases}
$$

Université de Liège

From the micro-scale to the meso-scale

- **Definition of Stochastic Volume Elements (SVEs)**
  - Poisson Voronoï tessellation realizations
    - SVE realization ω_j
  - Each grain ω_i is assigned material properties
    - $\mathbb{C}_{m^i}, \kappa_{m^i}, \alpha_{m^i,}$
    - Defined from silicon crystal properties
  - Each $\mathbb{C}_{m^i}$ is assigned a random orientation
    - Following XRD distributions
- **Stochastic homogenization**
  - Several SVE realizations
  - For each SVE $\quad \omega_j = \cup_i \omega_i$

$$\mathbb{C}_{m^i}, \kappa_{m^i}, \alpha_{m^i} \quad \forall i \quad \longrightarrow \quad \mathbb{C}_{M^j}, \kappa_{M^j}, \alpha_{M^j}$$

Computational homogenization

Samples of the meso-scale homogenized elasticity tensors

$\mathbb{C}_{m^i}, \kappa_{m^i}, \alpha_{m^i}$ (top left, green)
$\mathbb{C}_{m^i}, \kappa_{m^i}, \alpha_{m^i}$ (top, red)
$\mathbb{C}_{m^i}, \kappa_{m^i}, \alpha_{m^i}$ (right, purple)
$\mathbb{C}_{m^i}, \kappa_{m^i}, \alpha_{m^i}$ (bottom left)
$\mathbb{C}_{m^i}, \kappa_{m^i}, \alpha_{m^i}$ (bottom right)

$$\omega_j = \cup_i \omega_i$$

  - Homogenized material tensors not unique as statistical representativeness is lost*
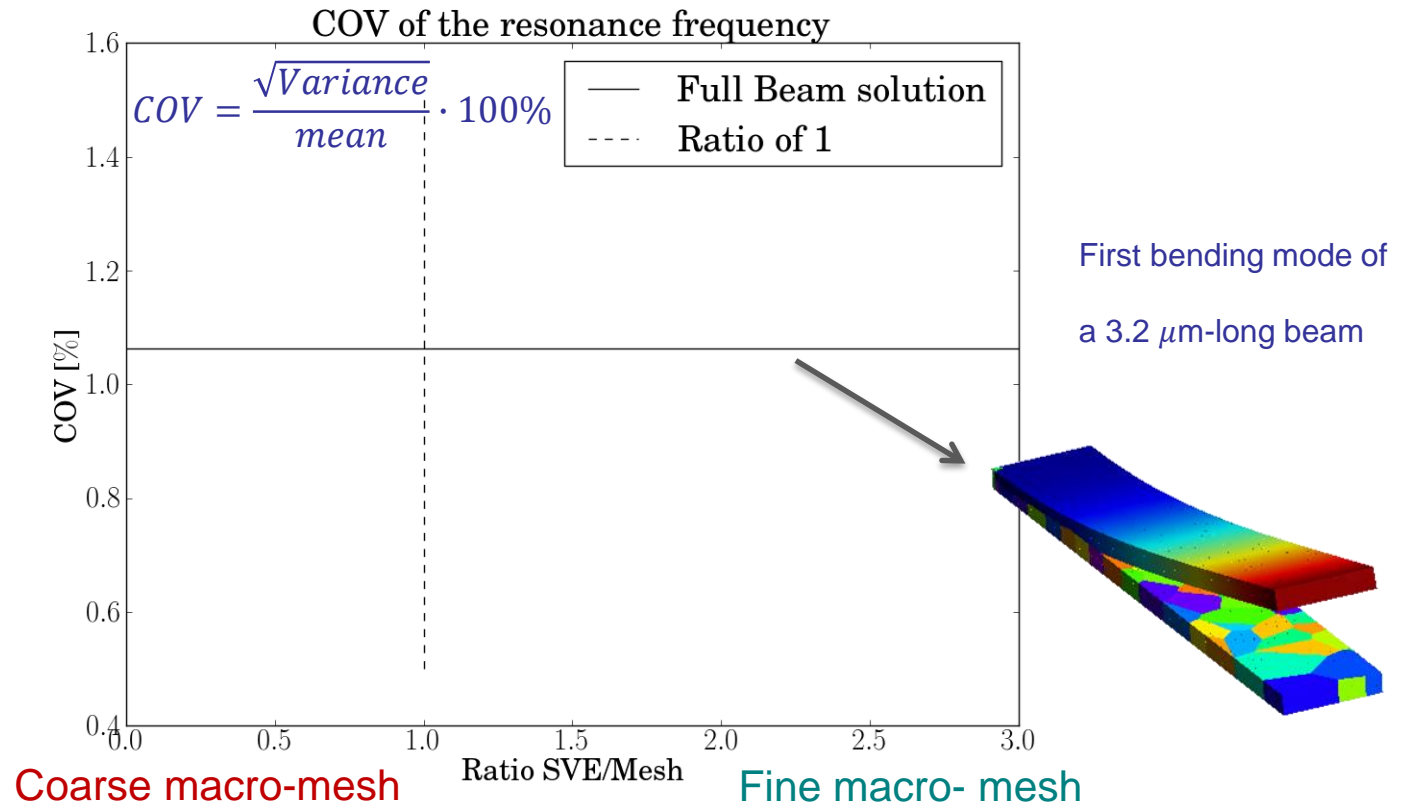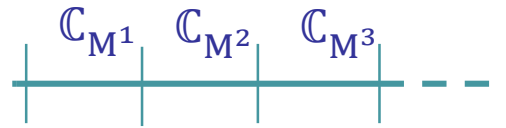
"C. Huet, 1990

- Distribution of the apparent meso-scale elasticity tensor $\mathbb{C}_M$

  – For large SVEs, the apparent tensor tends to the effective (and unique) one

$$COV = \frac{\sqrt{Variance}}{mean} \cdot 100\%$$
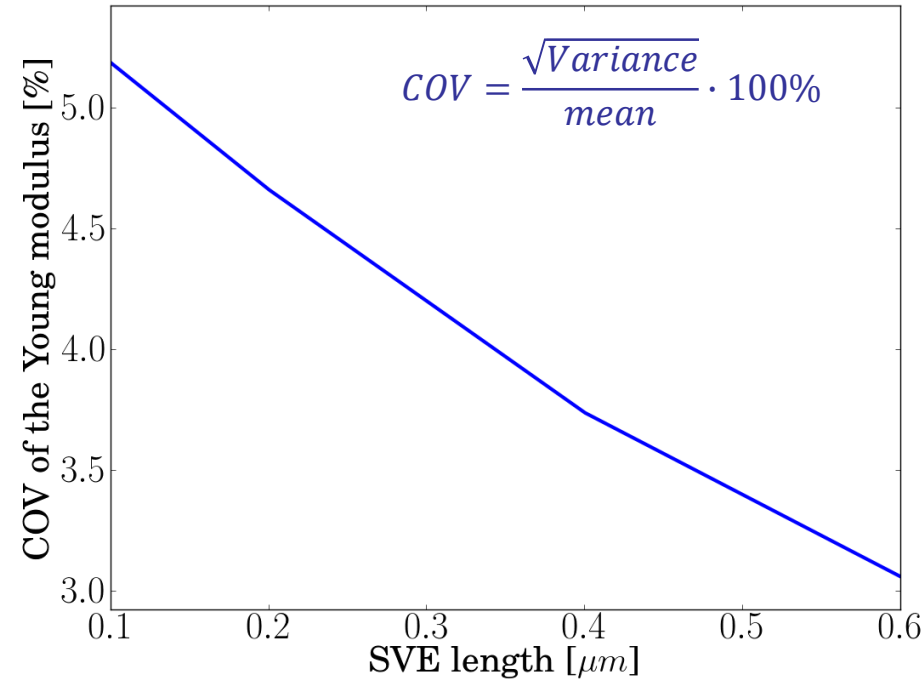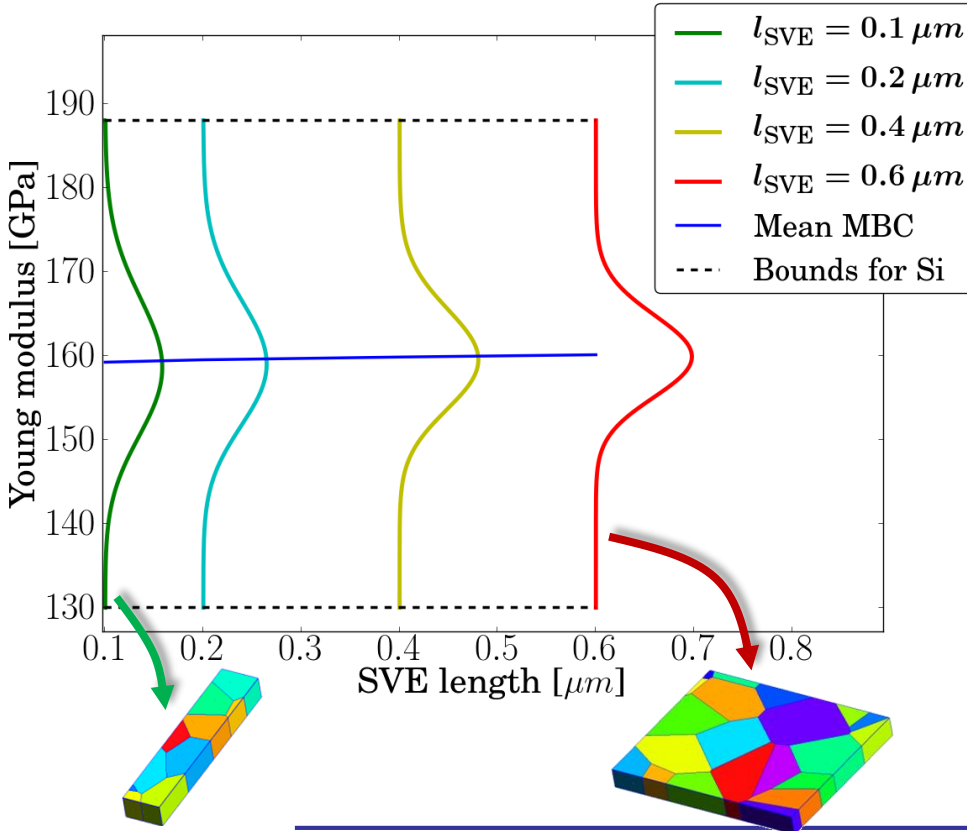
> The bounds do not depend on the SVE size but on the silicon elasticity tensor

> However, the larger the SVE, the lower the probability to be close to the bounds
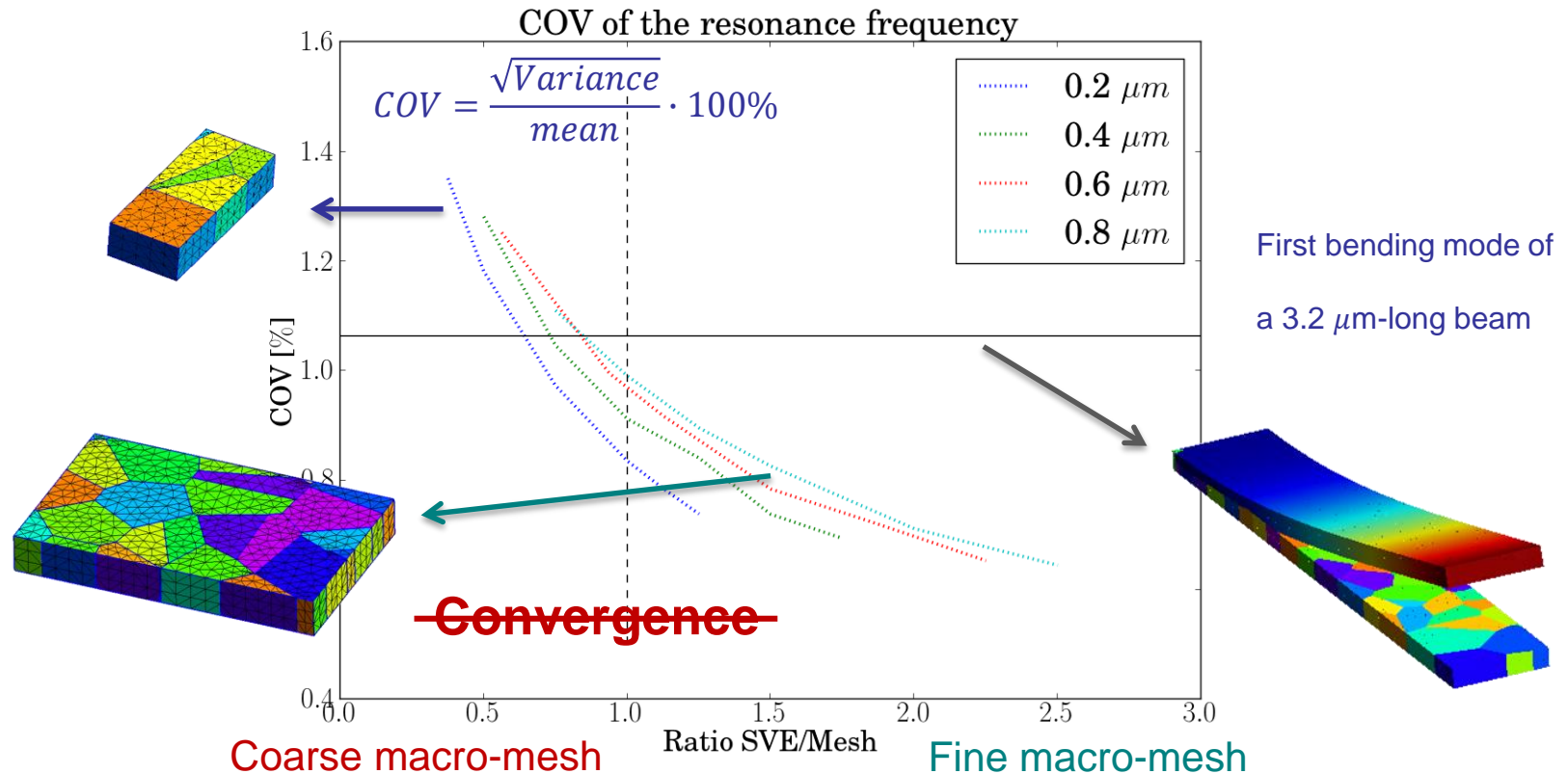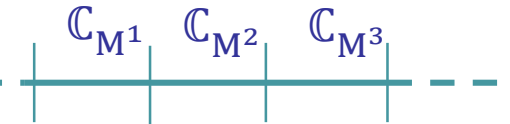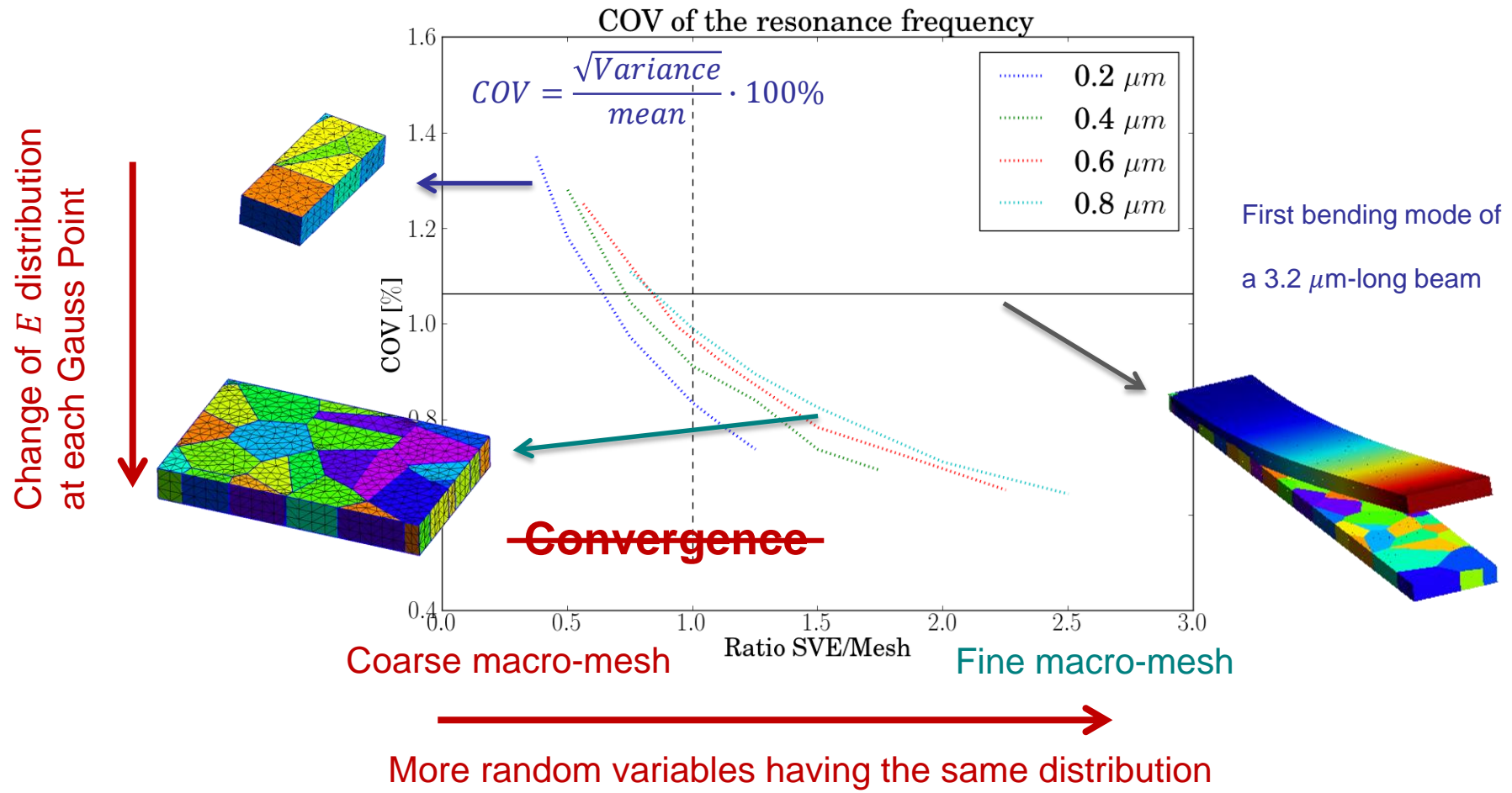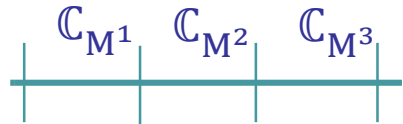
From the micro-scale to the meso-scale

- Use of the meso-scale distribution with macro-scale finite elements
  - Beam macro-scale finite elements
  - Use of the meso-scale distribution as a random variable
  - Monte-Carlo simulations

$\mathbb{C}_{M^1} \quad \mathbb{C}_{M^2} \quad \mathbb{C}_{M^3}$

COV of the resonance frequency

$$COV = \frac{\sqrt{Variance}}{mean} \cdot 100\%$$

— Full Beam solution
- - - Ratio of 1

First bending mode of

a 3.2 μm-long beam

COV [%]

Ratio SVE/Mesh

Coarse macro-mesh   Fine macro- mesh
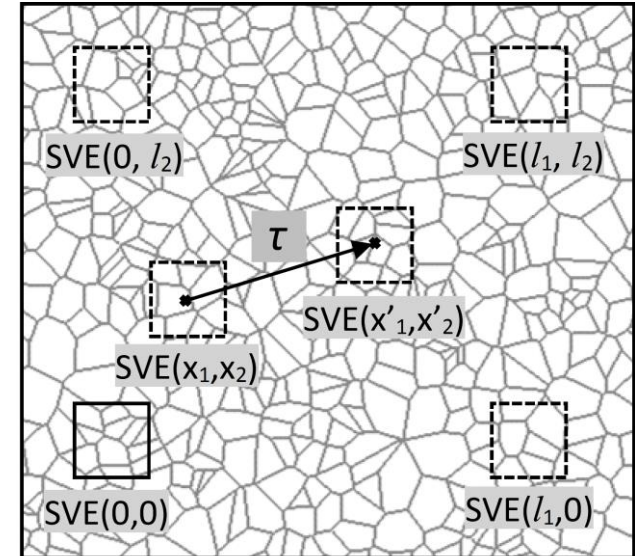
Université de Liège

From the micro-scale to the meso-scale

- Use of the meso-scale distribution with macro-scale finite elements
  - Beam macro-scale finite elements
  - Use of the meso-scale distribution as a random variable
  - Monte-Carlo simulations

$\mathbb{C}_{M^1} \quad \mathbb{C}_{M^2} \quad \mathbb{C}_{M^3}$


COV of the resonance frequency

$$COV = \frac{\sqrt{Variance}}{mean} \cdot 100\%$$

Legend:
- 0.2 μm
- 0.4 μm
- 0.6 μm
- 0.8 μm

COV [%]

Ratio SVE/Mesh

~~Convergence~~

Coarse macro-mesh   Fine macro-mesh

First bending mode of

a 3.2 μm-long beam

- No convergence: the macro-scale distribution (first resonance frequency) depends on SVE and mesh sizes

Université de Liège

From the micro-scale to the meso-scale

- Use of the meso-scale distribution with macro-scale finite elements
  - Beam macro-scale finite elements
  - Use of the meso-scale distribution as a random variable
  - Monte-Carlo simulations

$\mathbb{C}_{M^1}$ $\mathbb{C}_{M^2}$ $\mathbb{C}_{M^3}$

Change of E distribution at each Gauss Point

COV of the resonance frequency

$$COV = \frac{\sqrt{Variance}}{mean} \cdot 100\%$$

- 0.2 μm
- 0.4 μm
- 0.6 μm
- 0.8 μm

COV [%]

~~Convergence~~

Coarse macro-mesh

Ratio SVE/Mesh

Fine macro-mesh

First bending mode of

a 3.2 μm-long beam

More random variables having the same distribution

Université de Liège

From the micro-scale to the meso-scale

- Need for a meso-scale random field
    - Introduction of the (meso-scale) spatial correlation
        - Define large tessellations
        - SVEs extracted at different distances in each tessellation
    - Evaluate the spatial correlation between the components of the meso-scale material operators
    - For example, in 1D-elasticity
        - Young's modulus correlation

$$R_{E_x}(\tau) = \frac{\mathbb{E}\left[\left(E_x(x) - \mathbb{E}(E_x)\right)\left(E_x(x + \tau) - \mathbb{E}(E_x)\right)\right]}{\mathbb{E}\left[\left(E_x - \mathbb{E}(E_x)\right)^2\right]}$$

- Correlation length

$$L_{E_x} = \frac{\int_{-\infty}^{\infty} R_{E_x}(\tau)d\tau}{R_{E_x}(0)}$$

Université de Liège
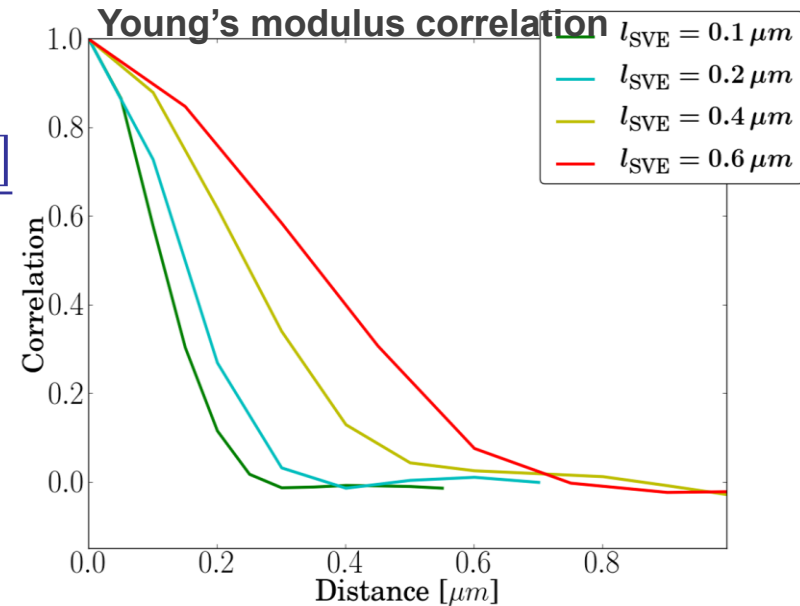
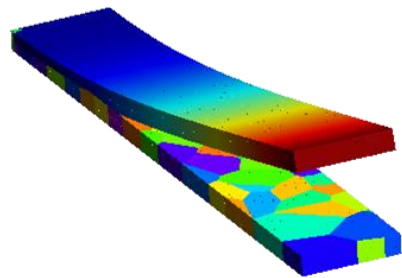- ## Need for a meso-scale random field (2)
  - The meso-scale random field is characterized by the correlation length L_{E_x}
  - The correlation length L_{E_x} depends on the SVE size

Random field with different SVEs sizes

$l_{\text{SVE}} = 0.1\ \mu m$
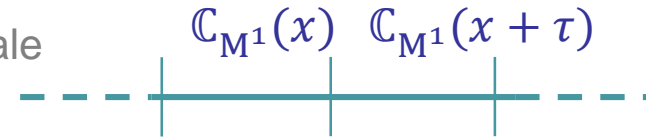
$l_{\text{SVE}} = 0.4\ \mu m$
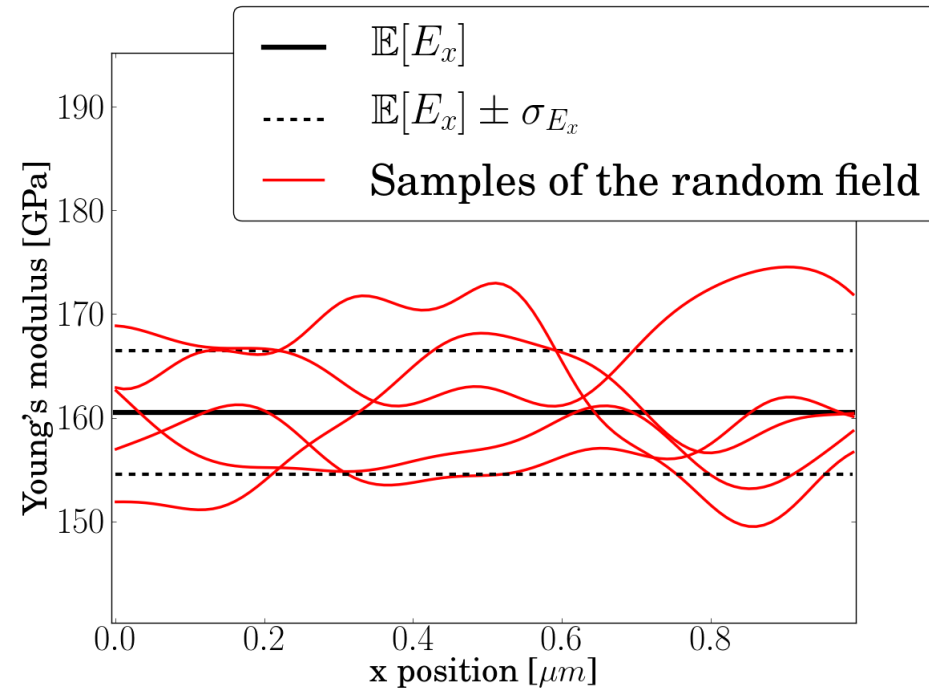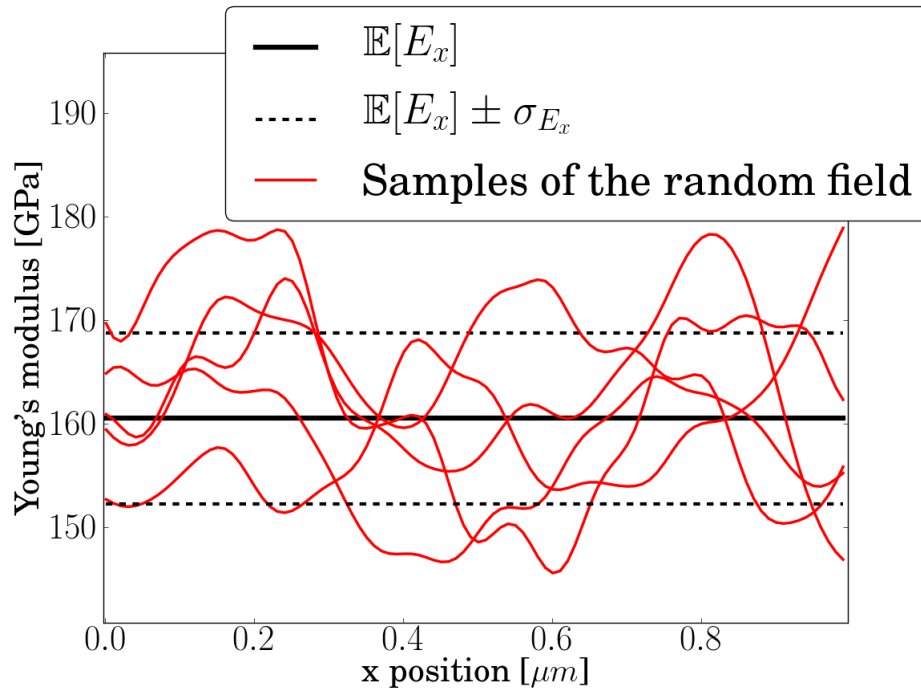
- ## Need for a meso-scale random field (3)

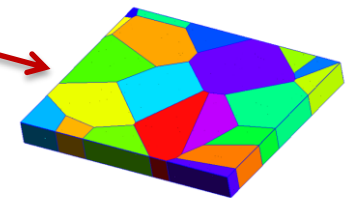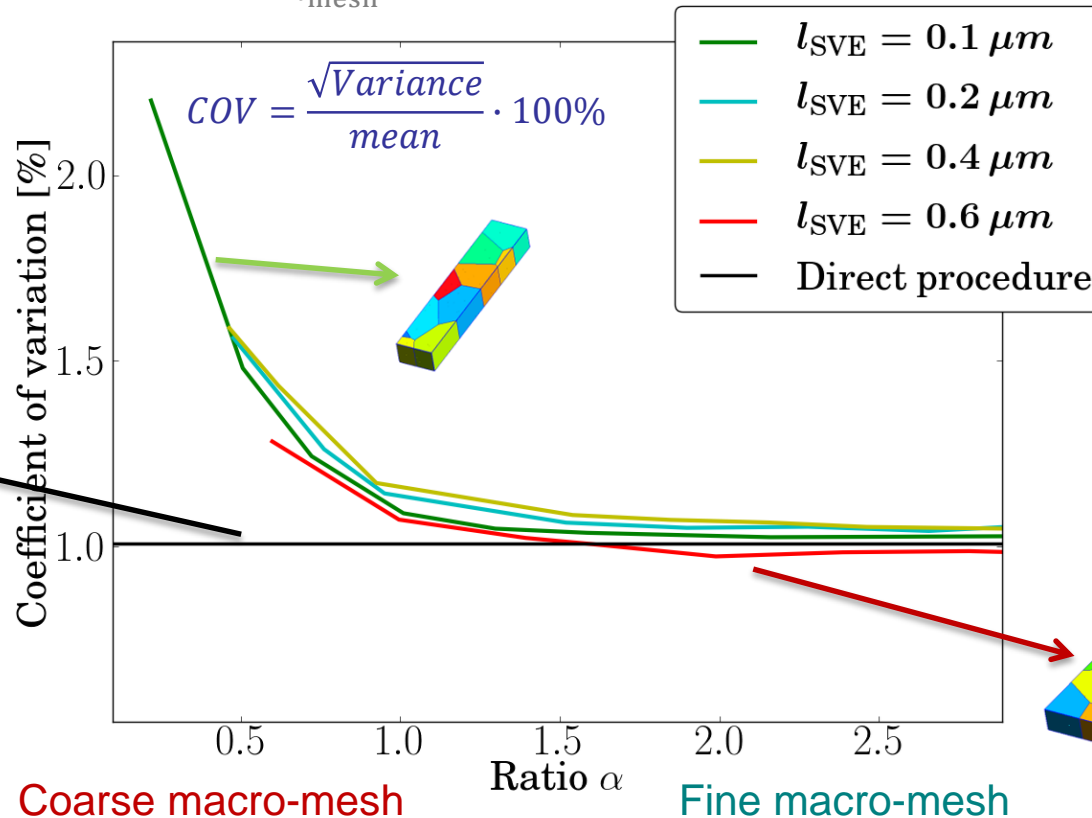 – Use of the meso-scale random field

    $\longrightarrow$ Monte-Carlo simulations at the macro-scale

  – Macro-scale beam elements of size l_{mesh}

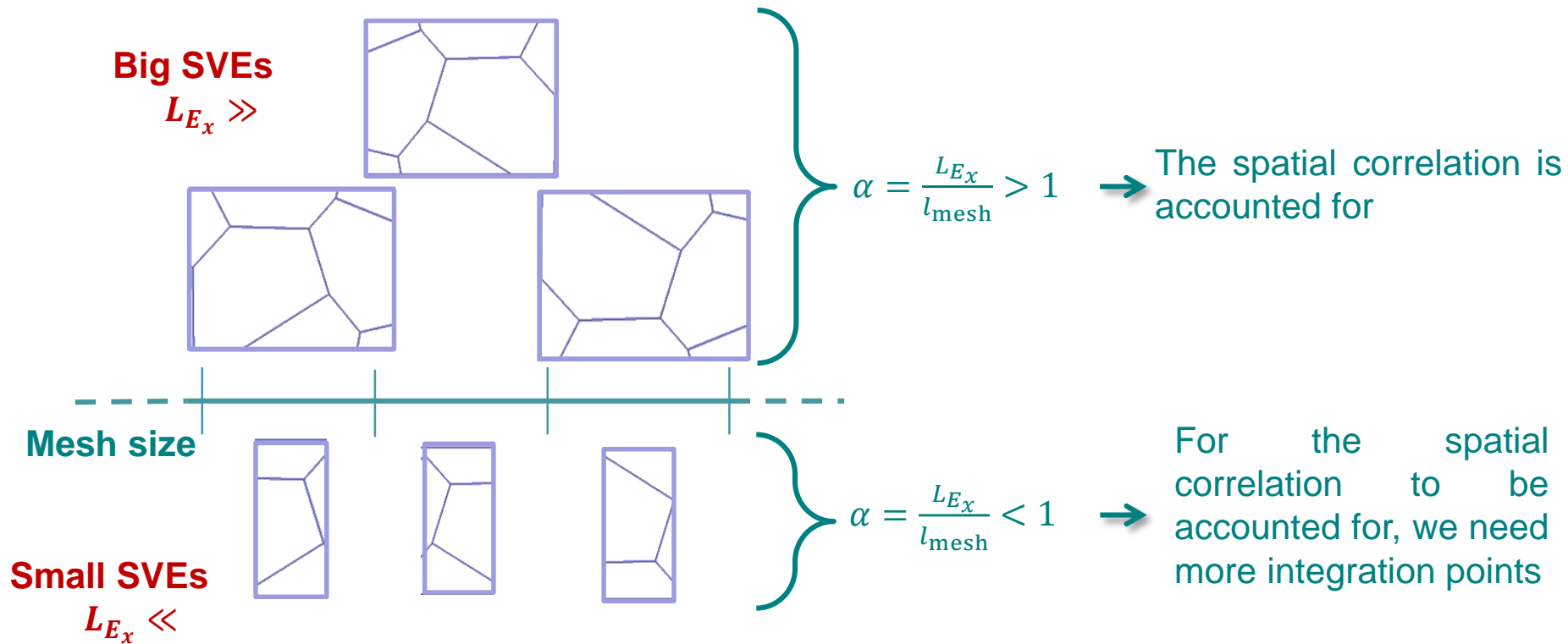 – Convergence in terms of $\alpha = \dfrac{L_{E_x}}{l_{\text{mesh}}}$

$$\mathbb{C}_{M^1}(x) \quad \mathbb{C}_{M^1}(x+\tau)$$

First bending mode of

a 3.2 μm-long beam

$$COV = \frac{\sqrt{Variance}}{mean} \cdot 100\%$$

Legend:
- $l_{\text{SVE}} = 0.1\,\mu m$
- $l_{\text{SVE}} = 0.2\,\mu m$
- $l_{\text{SVE}} = 0.4\,\mu m$
- $l_{\text{SVE}} = 0.6\,\mu m$
- Direct procedure

Coefficient of variation [%]

Ratio α

Coarse macro-mesh   Fine macro-mesh

From the micro-scale to the meso-scale

- Need for a meso-scale random field (3)

  - Effect of the ratio $\alpha = \frac{L_{E_x}}{l_{\text{mesh}}}$ (Only one gauss point in one element)

Big SVEs
$L_{E_x} \gg$

$\alpha = \frac{L_{E_x}}{l_{\text{mesh}}} > 1$ → The spatial correlation is accounted for

Mesh size

$\alpha = \frac{L_{E_x}}{l_{\text{mesh}}} < 1$ → For the spatial correlation to be accounted for, we need more integration points

Small SVEs
$L_{E_x} \ll$

- For extreme values of α:

  $\alpha \gg 1$: no more scale separation if $l_{\text{SVE}} \sim L_{\text{macro}}$

  $\alpha \ll 1$: loss of microstructural details if $l_{\text{SVE}} \sim L_{\text{micro}}$

Content

- Thermo-mechanical problems
  - Governing equations
  - Macro-scale stochastic finite element
  - Meso-scale volume elements
- From the micro-scale to the meso-scale
  - Thermo-mechanical homogenization
  - Definition of Stochastic Volume Elements (SVEs) & Stochastic homogenization
  - Need for a meso-scale random field
- **The meso-scale random field**
  - Definition of the thermo-mechanical meso-scale random field
  - Stochastic model of the random field: Spectral generator & non-Gaussian mapping
- From the meso-scale to the macro-scale
  - 3-Scale approach verification
  - Application to extract the quality factor

- Extension to stochastic-plate finite elements
  - Second-order stochastic homogenization
  - Rough Stochastic Volume Elements
  - Topology uncertainties effects

The meso-scale random field

- Use of the meso-scale distribution with stochastic (macro-scale) finite elements
    - Use of the meso-scale random field

        ⟶ Monte-Carlo simulations at the macro-scale

    - BUT we do not want to evaluate the random field from the stochastic homogenization

        for each simulation ⟶ Meso-scale random field from a generator

Stochastic model of meso-scale
elasticity tensors

Stochastic model

$$\mathbb{C}_{\mathrm{M}}(x + \tau, \theta)$$

$$\mathbb{C}_{\mathrm{M}}(x, \theta) \qquad \mathbb{C}_{\mathrm{M}}(x + 2\tau, \theta)$$

The meso-scale random field
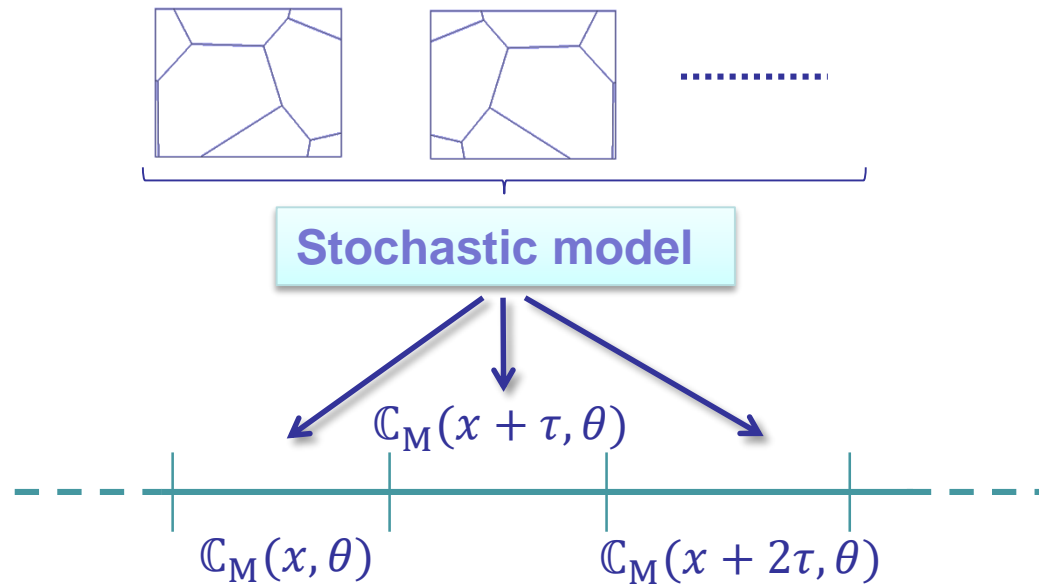
- Definition of the thermo-mechanical meso-scale random field
  - Elasticity tensor $\mathbb{C}_M(x,\theta)$ (matrix form $\boldsymbol{C}_M$) & thermal conductivity $\boldsymbol{\kappa}_M$ are bounded
    - Ensure existence of their inverse
    - Define lower bounds $\mathbb{C}_L$ and $\boldsymbol{\kappa}_L$ such that

$$\begin{cases} \boldsymbol{\varepsilon} : (\mathbb{C}_M - \mathbb{C}_L) : \boldsymbol{\varepsilon} > 0 & \forall \boldsymbol{\varepsilon} \\ \nabla\vartheta \cdot (\boldsymbol{\kappa}_M - \boldsymbol{\kappa}_L) \cdot \nabla\vartheta > 0 & \forall \nabla\vartheta \end{cases}$$

  - Use a Cholesky decomposition when semi-definite tensors are required

$$\begin{cases} \boldsymbol{C}_M(x,\boldsymbol{\theta}) = \boldsymbol{C}_L + \left(\overline{\mathcal{A}} + \mathcal{A}'(x,\boldsymbol{\theta})\right)^T \left(\overline{\mathcal{A}} + \mathcal{A}'(x,\boldsymbol{\theta})\right) \\ \boldsymbol{\kappa}_M(x,\boldsymbol{\theta}) = \boldsymbol{\kappa}_L + \left(\overline{\mathcal{B}} + \mathcal{B}'(x,\boldsymbol{\theta})\right)^T \left(\overline{\mathcal{B}} + \mathcal{B}'(x,\boldsymbol{\theta})\right) \\ \boldsymbol{\alpha}_{M_{ij}}(x,\boldsymbol{\theta}) = \overline{\mathcal{V}}^{(t)} + \mathcal{V}'^{(t)}(x,\boldsymbol{\theta}) \end{cases}$$

  - We define the homogenous zero-mean random field $\boldsymbol{\mathcal{V}}'(x,\boldsymbol{\theta})$, with as entries

    - Elasticity tensor $\mathcal{A}'(x,\boldsymbol{\theta}) \Rightarrow \boldsymbol{\mathcal{V}}'^{(1)} \ldots \boldsymbol{\mathcal{V}}'^{(21)}$,

    - Heat conductivity tensor $\mathcal{B}'(x,\boldsymbol{\theta}) \Rightarrow \boldsymbol{\mathcal{V}}'^{(22)} \ldots \boldsymbol{\mathcal{V}}'^{(27)}$

    - Thermal expansion tensors $\boldsymbol{\mathcal{V}}'^{(t)} \Rightarrow \boldsymbol{\mathcal{V}}'^{(28)} \ldots \boldsymbol{\mathcal{V}}'^{(33)}$

The meso-scale random field

- **Characterization of the meso-scale random field**

  - Generate large tessellation realizations

  - For each tessellation realization

    - Extract SVEs centred on $x + \tau$

    - For each SVE evaluate $\mathbb{C}_M(x + \tau), \kappa_M(x + \tau), \alpha_M(x + \tau)$

  - From the set of realizations $\mathbb{C}_M(x, \theta), \kappa_M(x, \theta), \alpha_M(x, \theta)$

    - Evaluate the bounds $\mathbb{C}_L$ and κ_L

    - Apply the Cholesky decomposition $\Rightarrow \mathcal{A}'(x, \theta), \mathcal{B}'(x, \theta)$

    - Fill the 33 entries of the zero-mean homogenous field $\mathcal{V}'(x, \theta)$

    - NB: for the thermal conductivity we use a grain-size dependent empirical relation

  - Compute the auto-/cross-correlation matrix
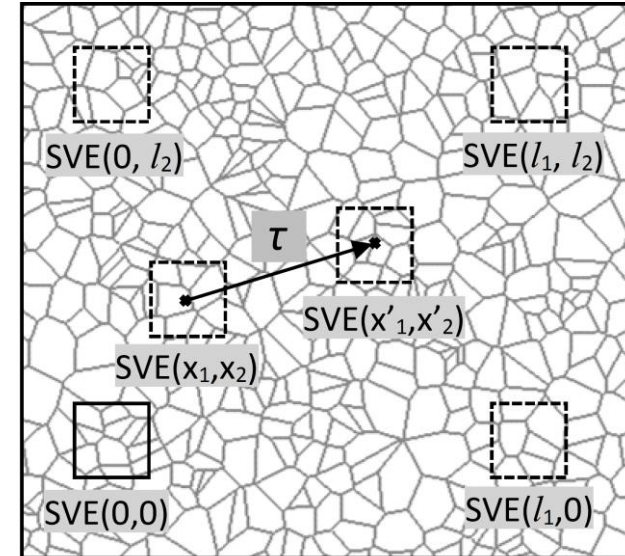
SVE(0, l_2)   SVE(l_1, l_2)

τ

SVE(x'$_1$,x'$_2$)

SVE(x$_1$,x$_2$)

SVE(0,0)   SVE(l_1,0)

$$R_{\mathcal{V}'}^{(rs)}(\tau) = \frac{\mathbb{E}\left[\left(\mathcal{V}'^{(r)}(x) - \mathbb{E}(\mathcal{V}'^{(r)})\right)\left(\mathcal{V}'^{(s)}(x + \tau) - \mathbb{E}(\mathcal{V}'^{(s)})\right)\right]}{\sqrt{\mathbb{E}\left[\left(\mathcal{V}'^{(r)} - \mathbb{E}(\mathcal{V}'^{(r)})\right)^2\right]\mathbb{E}\left[\left(\mathcal{V}'^{(s)} - \mathbb{E}(\mathcal{V}'^{(s)})\right)^2\right]}}$$

Université de Liège

The meso-scale random field

- Stochastic model of the meso-scale random field: Spectral generator*

  - Start from the auto-/cross-covariance matrix

  $$\tilde{R}_{\mathcal{V}'}^{(rs)}(\boldsymbol{\tau}) = \sigma_{\mathcal{V}'^{(r)}} \sigma_{\mathcal{V}'^{(s)}} R_{\mathcal{V}'}^{(rs)}(\boldsymbol{\tau}) = \mathbb{E}\left[\left(\mathcal{V}'^{(r)}(\boldsymbol{x}) - \mathbb{E}(\mathcal{V}'^{(r)})\right)\left(\mathcal{V}'^{(s)}(\boldsymbol{x}+\boldsymbol{\tau}) - \mathbb{E}(\mathcal{V}'^{(s)})\right)\right]$$

  - Evaluate the spectral density matrix from the periodized zero-padded matrix $\widetilde{\boldsymbol{R}}_{\mathcal{V}'}^{\mathrm{P}}(\boldsymbol{\tau})$

  $$S_{\mathcal{V}'}^{(rs)}[\boldsymbol{\omega}^{(m)}] = \sum_n \widetilde{R}_{\mathcal{V}'}^{\mathrm{P}\,(rs)}[\boldsymbol{\tau}^{(n)}] e^{-2\pi i \boldsymbol{\tau}^{(n)}\cdot\boldsymbol{\omega}^{(m)}} \quad \& \quad S_{\mathcal{V}'}[\boldsymbol{\omega}^{(m)}] = H_{\mathcal{V}'}[\boldsymbol{\omega}^{(m)}] H_{\mathcal{V}'}^*[\boldsymbol{\omega}^{(m)}]$$

    - $\boldsymbol{\omega}$ gathers the discrete frequencies

    - $\boldsymbol{\tau}$ gathers the discrete spatial locations

  - Generate a Gaussian random field $\mathcal{V}'(\boldsymbol{x},\boldsymbol{\theta})$

  $$\mathcal{V}'^{(r)}(\boldsymbol{x},\boldsymbol{\theta}) = \sqrt{2\Delta\omega}\,\Re\left(\sum_s \sum_m H_{\mathcal{V}'}^{(rs)}[\boldsymbol{\omega}^{(m)}] \eta^{(s,m)} e^{2\pi i\left(\boldsymbol{x}\cdot\boldsymbol{\omega}^{(m)}+\boldsymbol{\theta}^{(s,m)}\right)}\right)$$

    - $\boldsymbol{\eta}$ and $\boldsymbol{\theta}$ are independent random variables

  - Quid if a non-Gaussian distribution is sought?

*Shinozuka, M., Deodatis, G., 1988

The meso-scale random field

- ## Stochastic model of the meso-scale random field: non-Gaussian mapping*

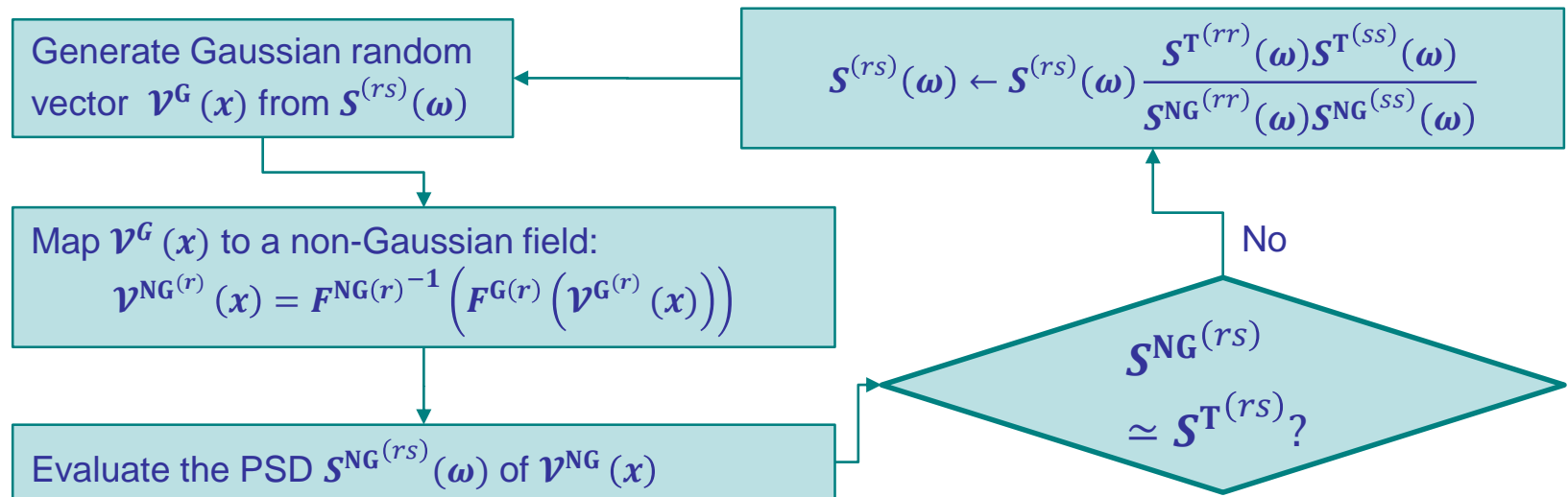 - Start from micro-sampling of the stochastic homogenization

    - The continuous form of the targeted PSD function

$$S^{\mathrm{T}(rs)}(\boldsymbol{\omega}) = \Delta\tau S_{\mathcal{V}'}^{(rs)}[\boldsymbol{\omega}^{(m)}] = \Delta\tau \sum_n \widetilde{R}_{\mathcal{V}'}^{\mathrm{P}}{}^{(rs)}[\boldsymbol{\tau}^{(n)}] e^{-2\pi i \boldsymbol{\tau}^{(n)} \cdot \boldsymbol{\omega}^{(m)}}$$

    - The targeted marginal distribution density function $F^{\mathrm{NG}(r)}$ of the random variable $\mathcal{V}'^{(r)}$

    - A marginal Gaussian distribution $F^{G(r)}$ of zero-mean and targeted variance $\sigma_{\mathcal{V}'^{(r)}}$

  - Iterate

Generate Gaussian random vector $\mathcal{V}^{\mathrm{G}}(x)$ from $S^{(rs)}(\boldsymbol{\omega})$	$S^{(rs)}(\boldsymbol{\omega}) \leftarrow S^{(rs)}(\boldsymbol{\omega}) \dfrac{S^{\mathrm{T}(rr)}(\boldsymbol{\omega}) S^{\mathrm{T}(ss)}(\boldsymbol{\omega})}{S^{\mathrm{NG}(rr)}(\boldsymbol{\omega}) S^{\mathrm{NG}(ss)}(\boldsymbol{\omega})}$

Map $\mathcal{V}^{\mathrm{G}}(x)$ to a non-Gaussian field:

$$\mathcal{V}^{\mathrm{NG}(r)}(x) = F^{\mathrm{NG}(r)-1}\left(F^{\mathrm{G}(r)}\left(\mathcal{V}^{\mathrm{G}(r)}(x) \right) \right)$$

Evaluate the PSD $S^{\mathrm{NG}(rs)}(\boldsymbol{\omega})$ of $\mathcal{V}^{\mathrm{NG}}(x)$

No

$$S^{\mathrm{NG}(rs)} \simeq S^{\mathrm{T}(rs)}?$$

*"Deodatis, G., Micaletti, R., 2001
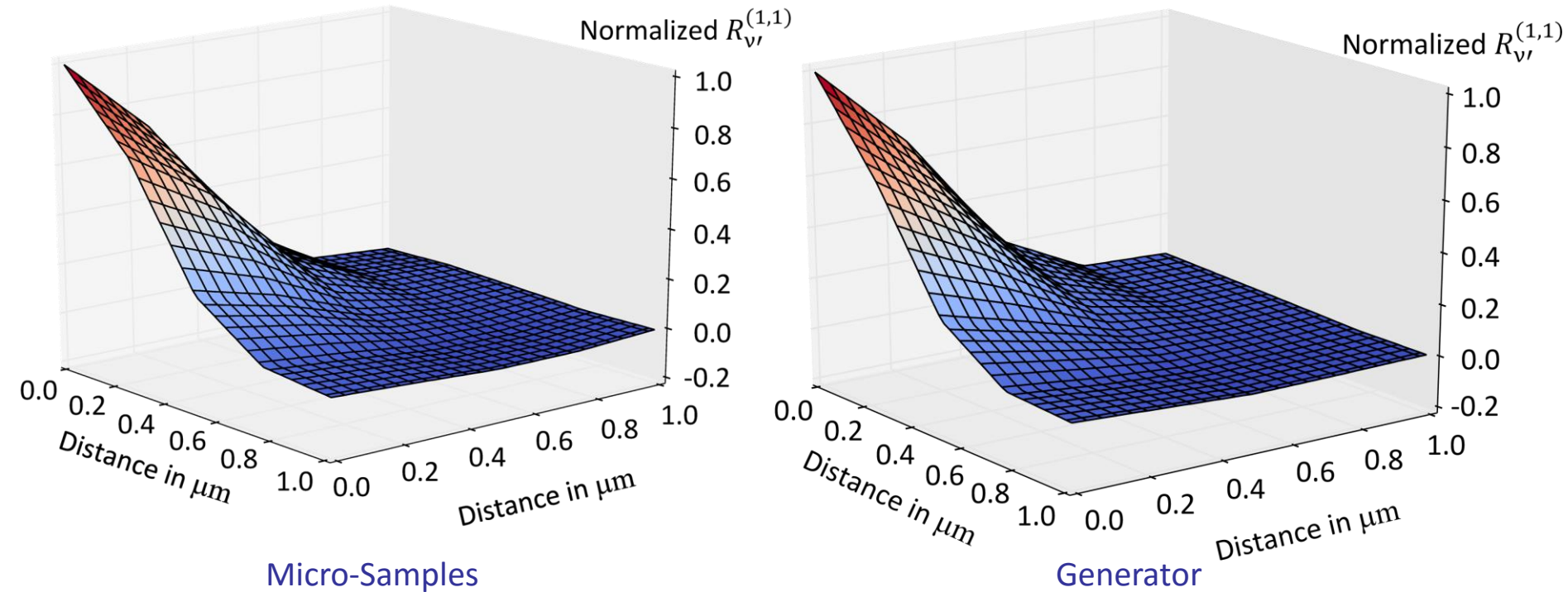
Université de Liège

The meso-scale random field

- **Polysilicon film deposited at 610 ºC**

  - SVE size of $0.5 \times 0.5\ \mu\mathrm{m}^2$

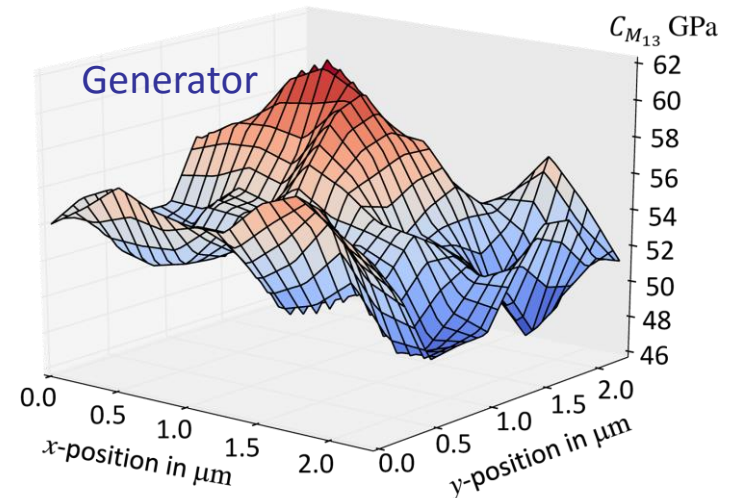 - Comparison between micro-samples and generated field PDF
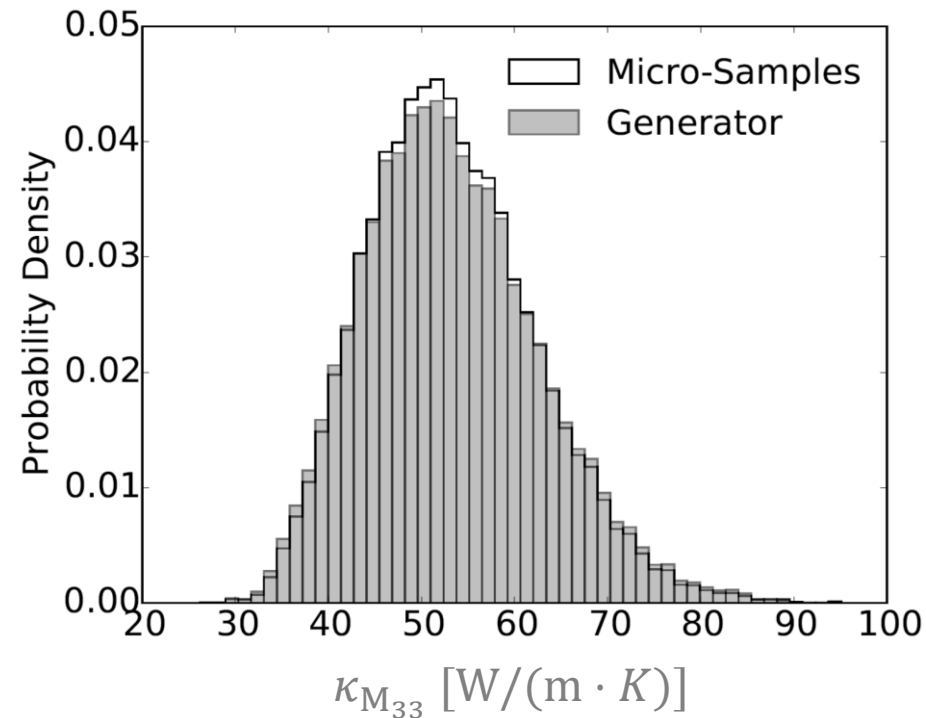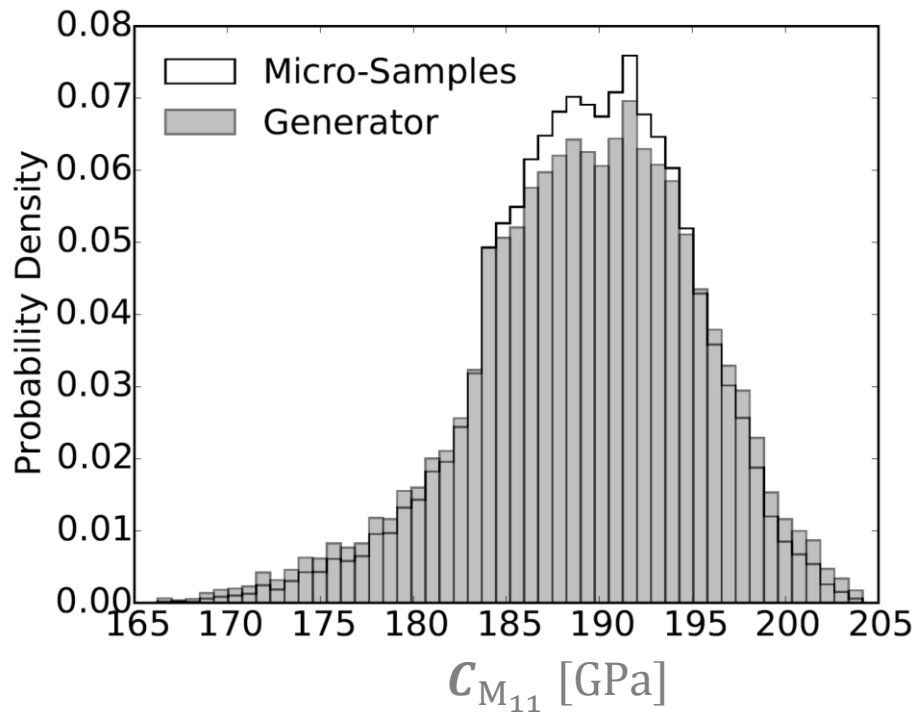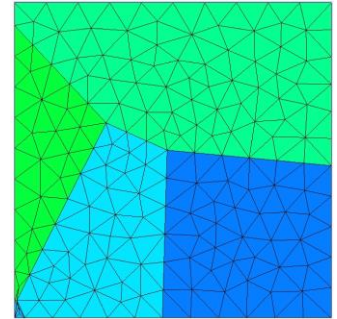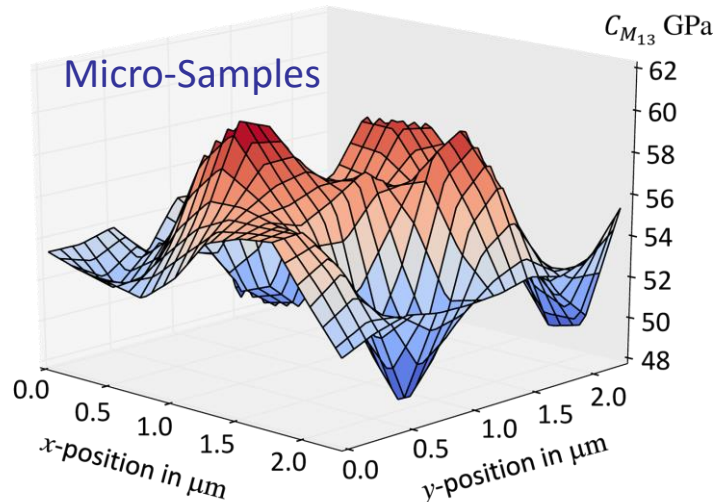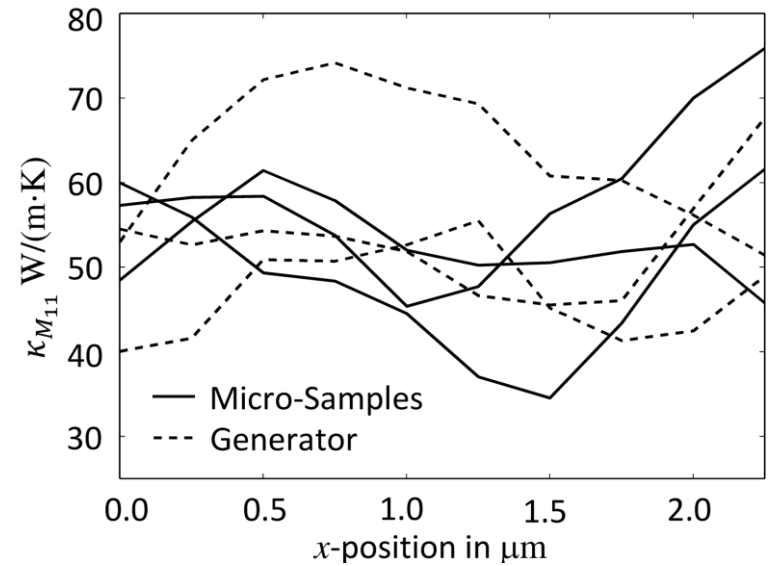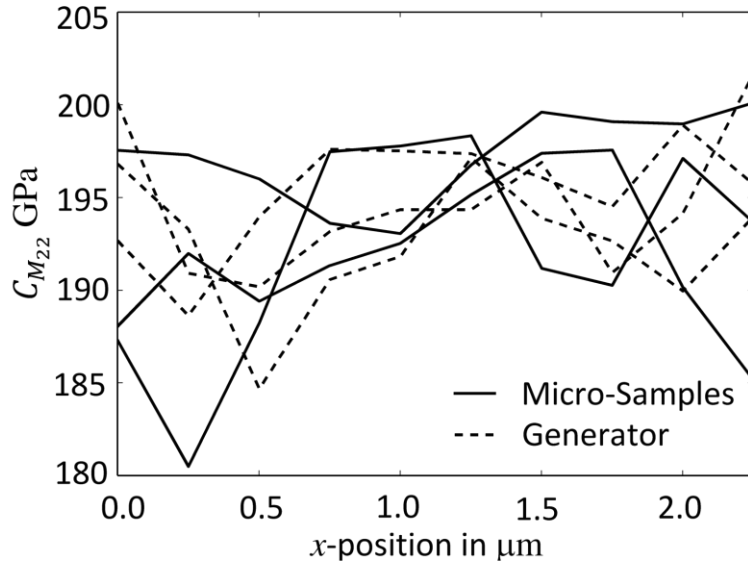
The meso-scale random field

- ## Polysilicon film deposited at 610 ºC (2)

  - Comparison between micro-samples and generated field cross-correlations

Micro-Samples

Generator

The meso-scale random field

- ## Polysilicon film deposited at 610 ºC (3)

  - Comparison between micro-samples and generated random field realizations

Content

- Thermo-mechanical problems
  – Governing equations
  – Macro-scale stochastic finite element
  – Meso-scale volume elements
- From the micro-scale to the meso-scale
  – Thermo-mechanical homogenization
  – Definition of Stochastic Volume Elements (SVEs) & Stochastic homogenization
  – Need for a meso-scale random field
- The meso-scale random field
  – Definition of the thermo-mechanical meso-scale random field
  – Stochastic model of the random field: Spectral generator & non-Gaussian mapping
- **From the meso-scale to the macro-scale**
  – 3-Scale approach verification
  – Application to extract the quality factor

- Extension to stochastic-plate finite elements
  – Second-order stochastic homogenization
  – Rough Stochastic Volume Elements
  – Topology uncertainties effects
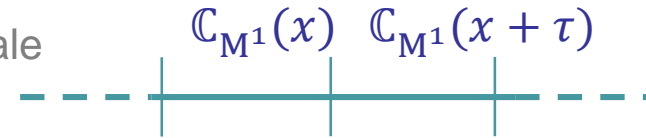
From the meso-scale to the macro-scale

- **3-Scale approach verification with direct Monte-Carlo simulations**

  – Use of the meso-scale random field
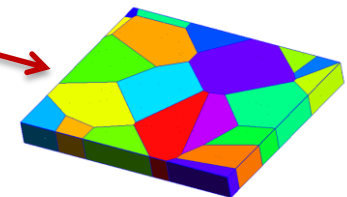
  $\longrightarrow$ Monte-Carlo simulations at the macro-scale

  $\mathbb{C}_{M^1}(x) \quad \mathbb{C}_{M^1}(x + \tau)$

  – Macro-scale beam elements of size l_{mesh}

  – Convergence in terms of $\alpha = \dfrac{l_{E_x}}{l_{\mathrm{mesh}}}$

$$COV = \frac{\sqrt{Variance}}{mean} \cdot 100\%$$

Legend:
- $l_{\mathrm{SVE}} = 0.1\,\mu m$
- $l_{\mathrm{SVE}} = 0.2\,\mu m$
- $l_{\mathrm{SVE}} = 0.4\,\mu m$
- $l_{\mathrm{SVE}} = 0.6\,\mu m$
- Direct procedure

Coefficient of variation [%]

Ratio α

Coarse macro-mesh   Fine macro-mesh

First bending mode of

a 3.2 μm-long beam
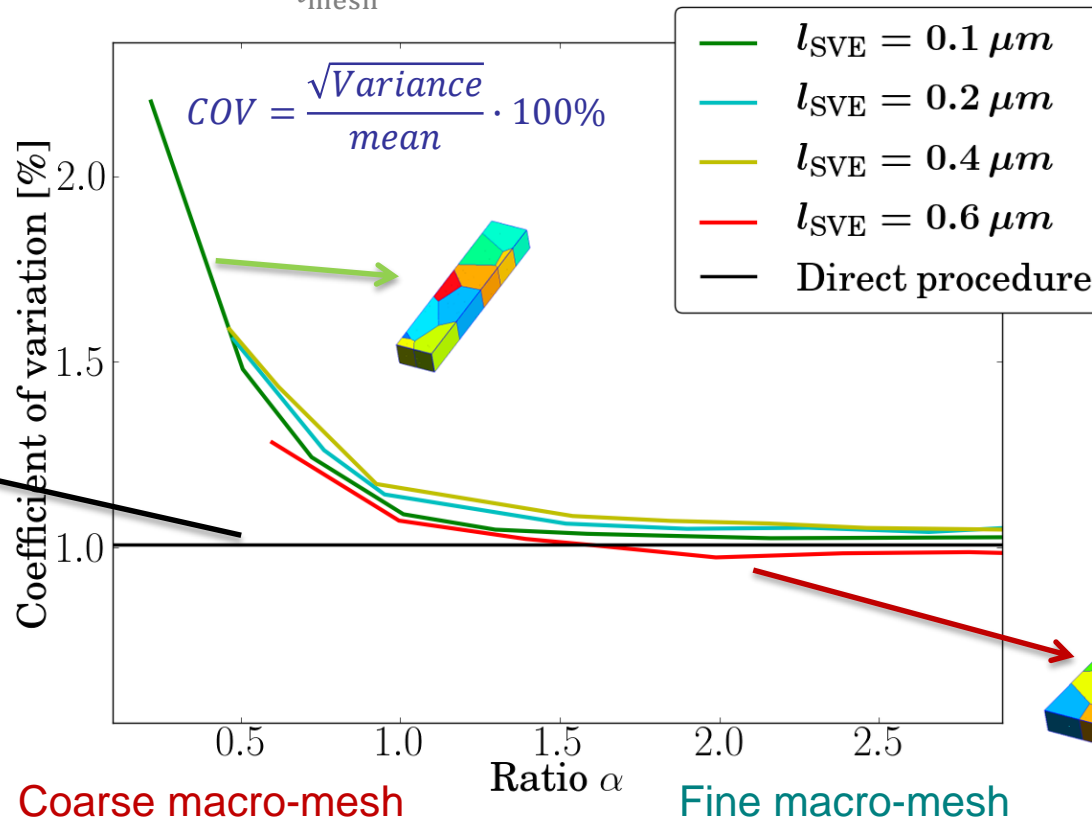
- 3-Scale approach verification ($\alpha \sim 2$) with direct Monte-Carlo simulations

  – First bending mode

First bending mode of
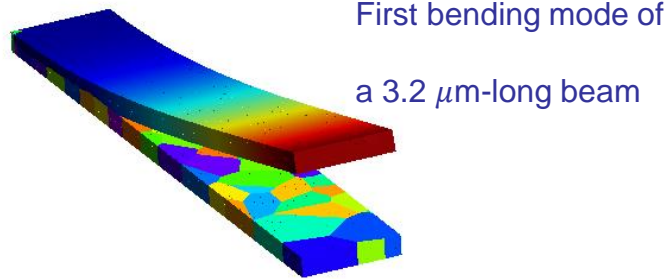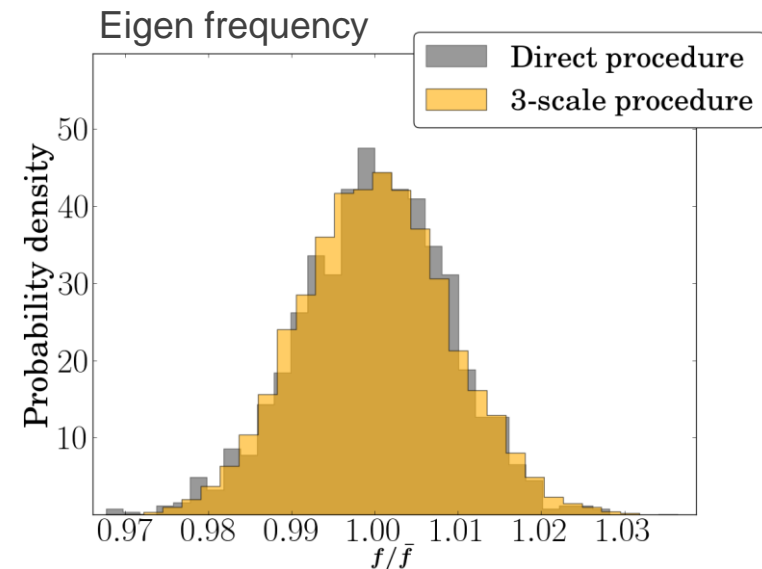
a 3.2 μm-long beam

  – Second bending mode

Second bending mode of

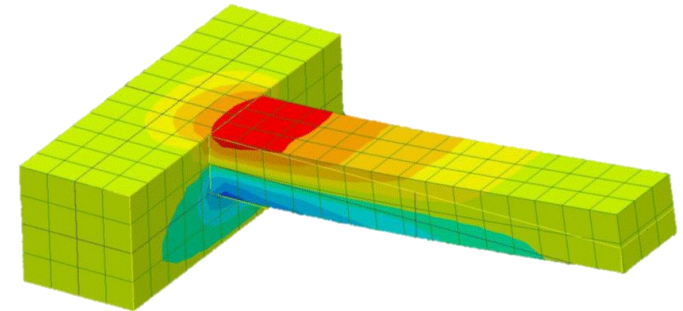a 3.2 μm-long beam

From the meso-scale to the macro-scale
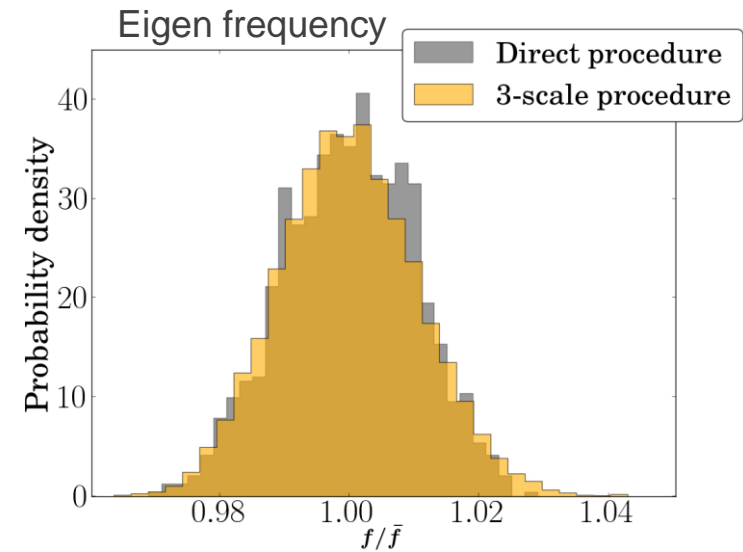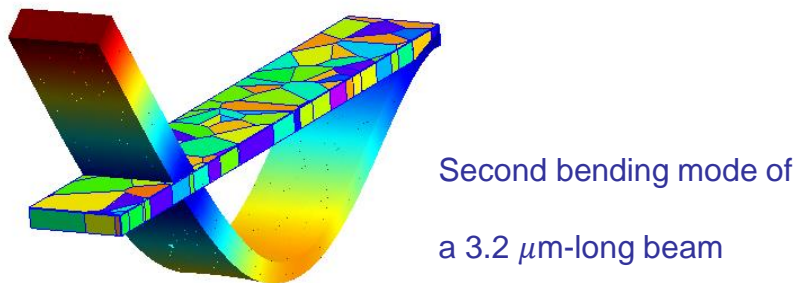
- **Quality factor**
  - Micro-resonators
    - Temperature changes with compression/traction
    - Energy dissipation

  - Eigen values problem
    - Governing equations

$$\begin{bmatrix} \mathbf{M} & \mathbf{0} \\ \mathbf{0} & \mathbf{0} \end{bmatrix}\begin{bmatrix} \ddot{\mathbf{u}} \\ \ddot{\boldsymbol{\vartheta}} \end{bmatrix} + \begin{bmatrix} \mathbf{0} & \mathbf{0} \\ \mathbf{D}_{u\vartheta}(\boldsymbol{\theta}) & \mathbf{D}_{\vartheta\vartheta} \end{bmatrix}\begin{bmatrix} \dot{\mathbf{u}} \\ \dot{\boldsymbol{\vartheta}} \end{bmatrix} + \begin{bmatrix} \mathbf{K}_{uu}(\boldsymbol{\theta}) & \mathbf{K}_{u\vartheta}(\boldsymbol{\theta}) \\ \mathbf{0} & \mathbf{K}_{\vartheta\vartheta}(\boldsymbol{\theta}) \end{bmatrix}\begin{bmatrix} \mathbf{u} \\ \boldsymbol{\vartheta} \end{bmatrix} = \begin{bmatrix} F_u \\ F_\vartheta \end{bmatrix}$$

    - Free vibrating problem

$$\begin{bmatrix} \mathbf{u}(t) \\ \boldsymbol{\vartheta}(t) \end{bmatrix} = \begin{bmatrix} \mathbf{u_0} \\ \boldsymbol{\vartheta_0} \end{bmatrix} e^{i\omega t}$$

$$\begin{bmatrix} -\mathbf{K}_{uu}(\boldsymbol{\theta}) & -\mathbf{K}_{u\vartheta}(\boldsymbol{\theta}) & \mathbf{0} \\ \mathbf{0} & -\mathbf{K}_{\vartheta\vartheta}(\boldsymbol{\theta}) & \mathbf{0} \\ \mathbf{0} & \mathbf{0} & \mathbf{I} \end{bmatrix}\begin{bmatrix} \mathbf{u} \\ \boldsymbol{\vartheta} \\ \dot{\mathbf{u}} \end{bmatrix} = i\omega \begin{bmatrix} \mathbf{0} & \mathbf{0} & \mathbf{M} \\ \mathbf{D}_{\vartheta u}(\boldsymbol{\theta}) & \mathbf{D}_{\vartheta\vartheta} & \mathbf{0} \\ \mathbf{I} & \mathbf{0} & \mathbf{0} \end{bmatrix}\begin{bmatrix} \mathbf{u} \\ \boldsymbol{\vartheta} \\ \dot{\mathbf{u}} \end{bmatrix}$$
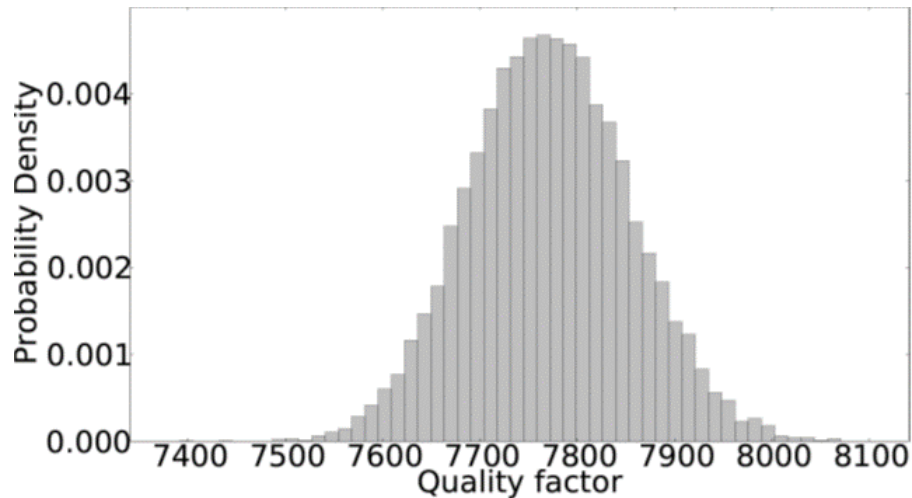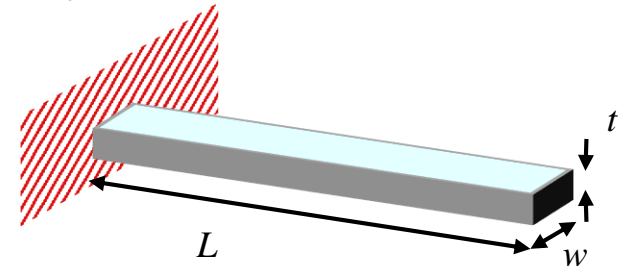
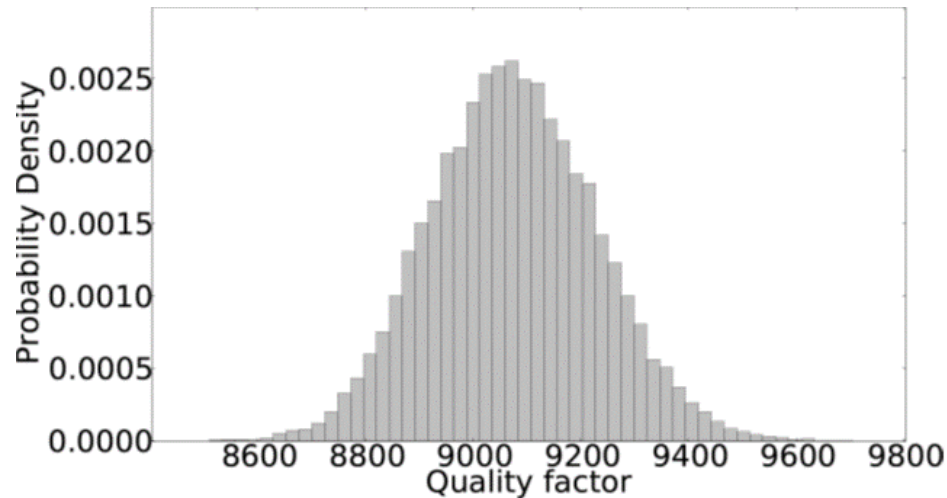 - Quality factor
    - From the dissipated energy per cycle
    - $Q^{-1} = \dfrac{2|\Im\omega|}{\sqrt{(\Im\omega)^2 + (\Re\omega)^2}}$

From the meso-scale to the macro-scale

- Application of the 3-Scale method to extract the quality factor distribution
  - Perfectly clamped micro-resonator
    - Different sizes easily considered
  - Meso-scale random fields
    - From stochastic homogenization
    - Generated for different deposition temperatures
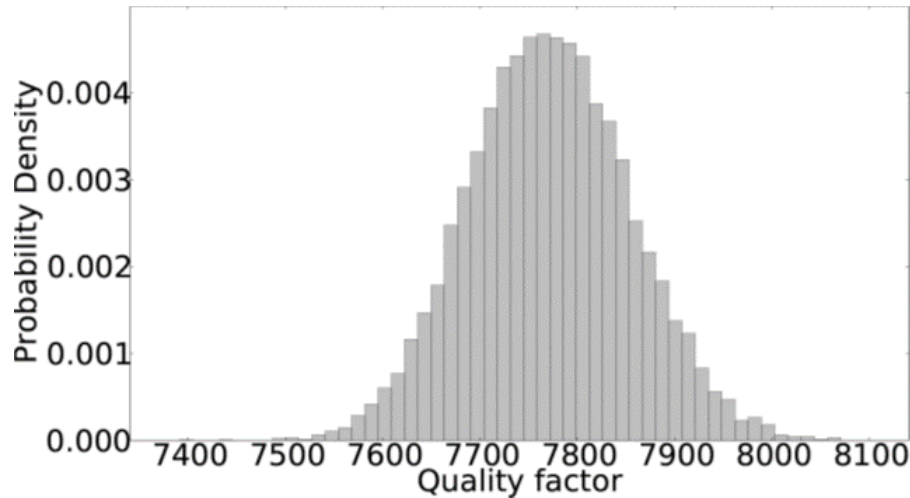 - Effect of the deposition temperature

15 x 3 x 2 μm^3-beam,

deposited at 610 ºC

15 x 3 x 2 μm^3-beam,

deposited at 630 ºC

From the meso-scale to the macro-scale

- Application of the 3-Scale method to extract the quality factor distribution (2)

    – Perfectly clamped micro-resonator
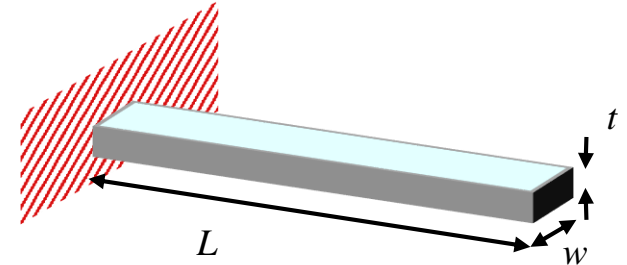
    – Effect of the geometry

15 x 3 x 2 μm^3-beam,

deposited at 610 ºC
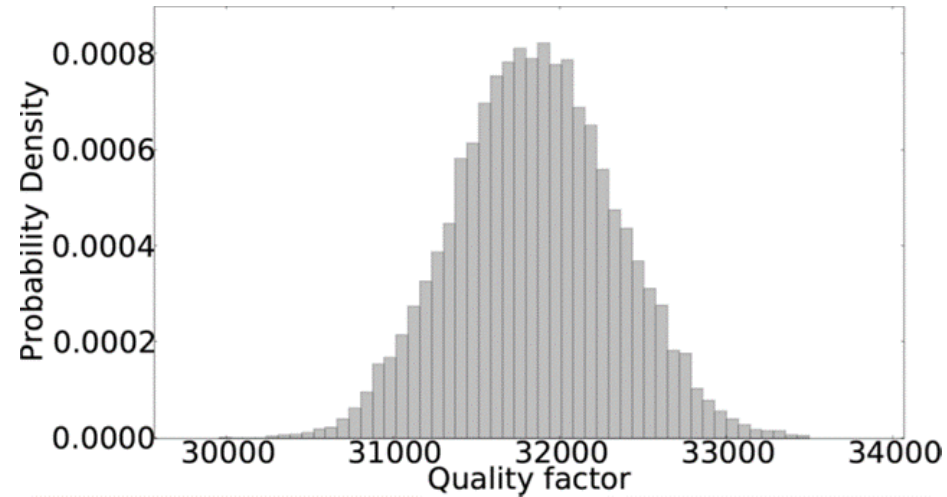
15 x 3 x 1 μm^3-beam,

deposited at 610 ºC

From the meso-scale to the macro-scale

- Application of the 3-Scale method to extract the quality factor distribution (3)
  - 3D models readily available
  - The effect of the anchor can be studied
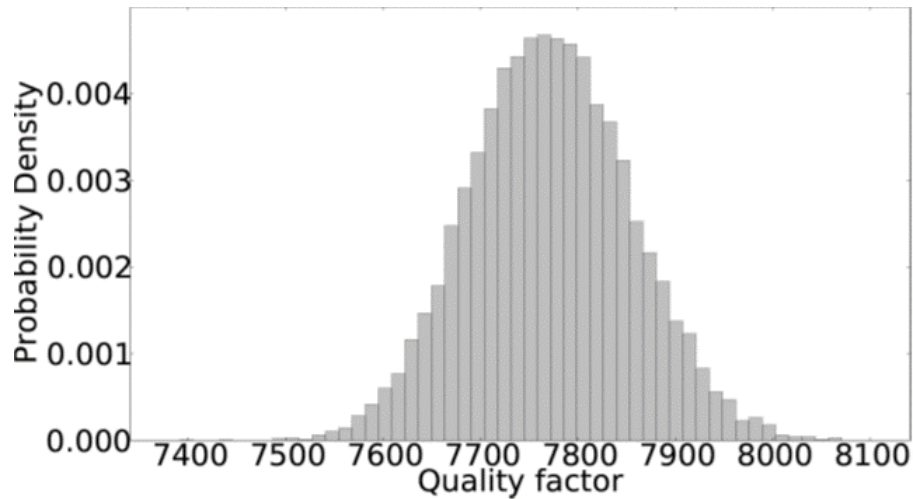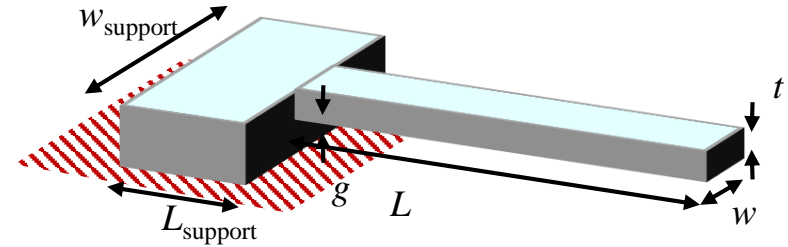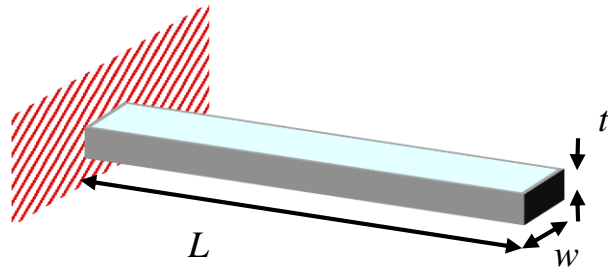
$15 \times 3 \times 2 \ \mu m^3$-beam, deposited at 610 ºC
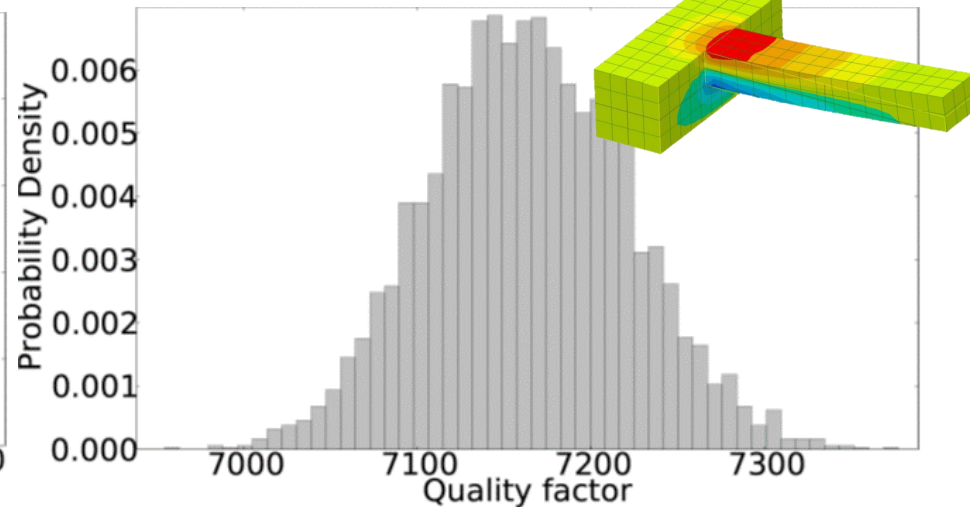
$15 \times 3 \times 2 \ \mu m^3$-beam & anchor, deposited at 610 ºC

CM3

Content

- Thermo-mechanical problems
    - Governing equations
    - Macro-scale stochastic finite element
    - Meso-scale volume elements
- From the micro-scale to the meso-scale
    - Thermo-mechanical homogenization
    - Definition of Stochastic Volume Elements (SVEs) & Stochastic homogenization
    - Need for a meso-scale random field
- The meso-scale random field
    - Definition of the thermo-mechanical meso-scale random field
    - Stochastic model of the random field: Spectral generator & non-Gaussian mapping
- From the meso-scale to the macro-scale
    - 3-Scale approach verification
    - Application to extract the quality factor

- Extension to stochastic-plate finite elements
    - Second-order stochastic homogenization
    - Rough Stochastic Volume Elements
    - Topology uncertainties effects

Extension to stochastic-plate finite elements

- How to account for the surface topology uncertainties?
  - Upper surface topology by AFM measurements on 2 μm-thick poly-silicon films
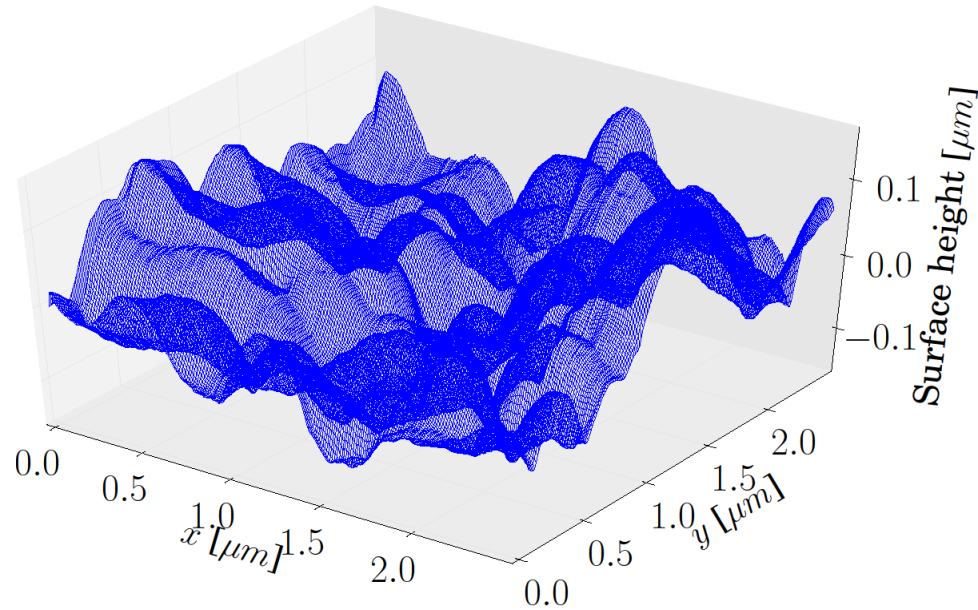
Temperature [°C]	580	610	630	650
Std deviation [nm]	35.6	60.3	90.7	88.3

AFM data provided by IMT Bucharest, Rodica Voicu, Angela Baracu, Raluca Muller

Stochastic multi-scale method for Kirchhoff-Love (KL) plates

- **Macro-scale**
  - Stochastic Kirchhoff-Love plates

- **Meso-scale**
  - Rough Stochastic Volume Elements (RSVEs)
  - Profiles from AFM

- **Scale transition**
  - Downscaling
    - In plane deformation $\boldsymbol{\varepsilon}_\mathrm{M}$
    - Curvature/torsion $\boldsymbol{\kappa}_\mathrm{M}$
  - Upscaling
    - In-plane stress per unit length $\tilde{\boldsymbol{n}}_\mathrm{M}$
    - Bending moment/torque per unit length $\tilde{\boldsymbol{m}}_\mathrm{M}$

- **Micro-scale**
  - Grain size/orientation distributions
  - From SEM/XRD measurements

$\tilde{\boldsymbol{n}}_\mathrm{M}, \mathbb{C}_{\mathrm{M}_1}, \mathbb{C}_{\mathrm{M}_2}$

$\tilde{\boldsymbol{m}}_\mathrm{M}, \mathbb{C}_{\mathrm{M}_3}, \mathbb{C}_{\mathrm{M}_4}$

$\boldsymbol{\varepsilon}_\mathrm{M}, \boldsymbol{\kappa}_\mathrm{M}$

Meso-scale BVP resolution

$\mathscr{A}$

$\bar{h}/2$

$\boldsymbol{\omega} = \cup_i \boldsymbol{\omega}_i$
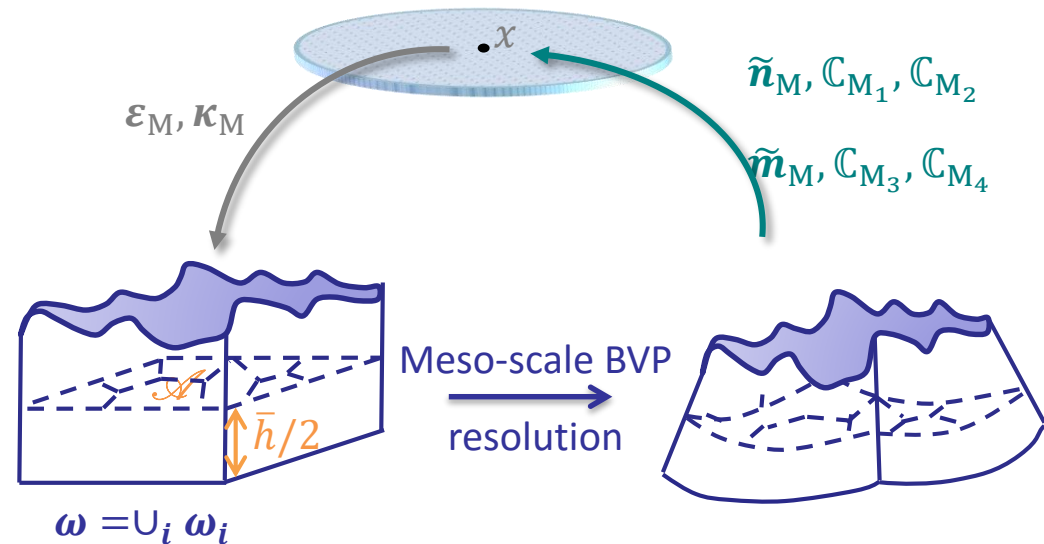
Stochastic multi-scale method for Kirchhoff-Love (KL) plates

- **Rough Stochastic Volume Element**
  - Poisson Voronoï tessellation realizations
    - From topology generator
    - Use of AFM measurements
  - Extraction of volume elements ω_j
    - Each grain ω_i is assigned material properties $\mathbb{C}_{m^i}$
    - Defined from silicon crystal properties
  - Each $\mathbb{C}_{m^i}$ is assigned a random orientation
    - Uniformly distributed
    - Following XRD distributions
  - Governing equations
    - Classical continuum mechanics

$$\begin{cases} \nabla \cdot \boldsymbol{\sigma}_{\mathbf{m}} = 0 \\ \\ \boldsymbol{\varepsilon}_{\mathrm{m}_{ij}} = \dfrac{\boldsymbol{u}_{\mathrm{m}_{i,j}} + \boldsymbol{u}_{\mathrm{m}_{i,j}}}{2} \end{cases}$$

  - Anisotropic grains
$$\boldsymbol{\sigma}_{\mathrm{m}}^{i} = \mathbb{C}_{\mathrm{m}^i} : \boldsymbol{\varepsilon}_{\mathrm{m}}^{i}$$

$\mathbb{C}_{m^i}$ $\mathbb{C}_{m^i}$ $\mathbb{C}_{m^i}$

$\omega_j = \cup_i \omega_i$
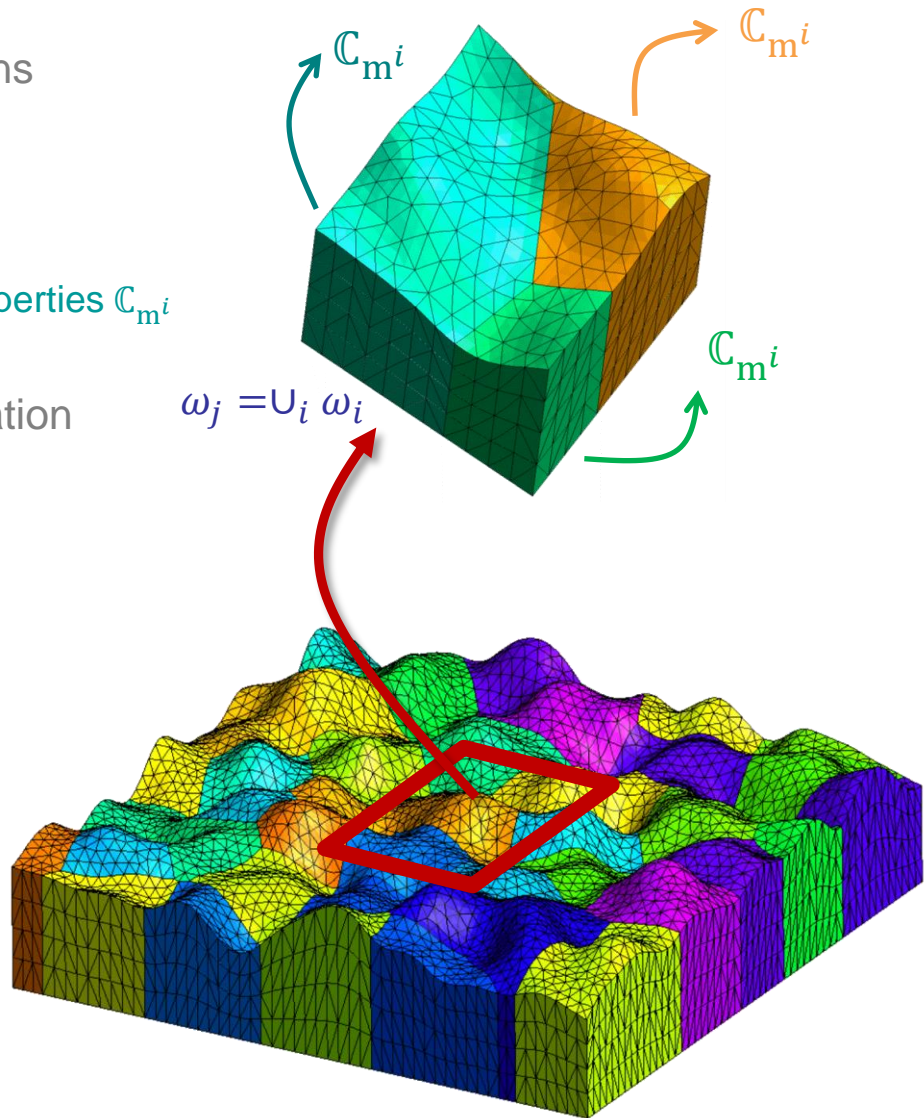
Stochastic multi-scale method for Kirchhoff-Love (KL) plates

- Second-order homogenization
  - Upscaling

$$
\begin{cases}
\widetilde{\boldsymbol{n}}_{\mathrm{M}} = \mathbb{C}_{\mathrm{M}_1} : \boldsymbol{\varepsilon}_{\mathrm{M}} + \mathbb{C}_{\mathrm{M}_2} : \boldsymbol{\kappa}_{\mathrm{M}} \\[2mm]
\widetilde{\boldsymbol{m}}_{\mathrm{M}} = \mathbb{C}_{\mathrm{M}_3} : \boldsymbol{\varepsilon}_{\mathrm{M}} + \mathbb{C}_{\mathrm{M}_4} : \boldsymbol{\kappa}_{\mathrm{M}}
\end{cases}
$$

- Stochastic homogenization
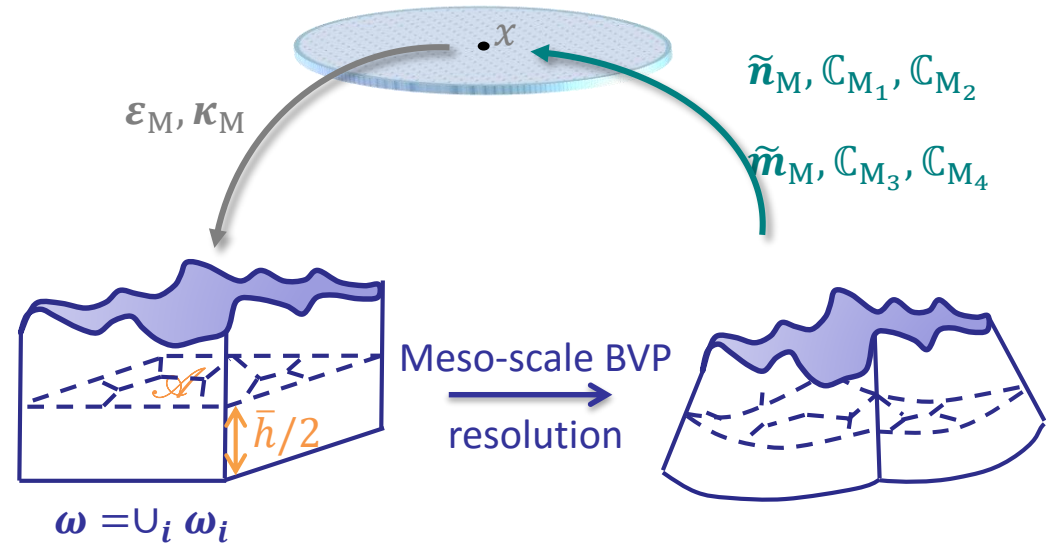
  - Several SVE realizations
  - For each SVE $\quad \omega_j = \cup_i \omega_i$

$\mathbb{C}_{\mathrm{m}^i} \ \forall i \quad \longrightarrow \quad \mathbb{C}_{\mathrm{M}_1^j}, \mathbb{C}_{\mathrm{M}_2^j}, \mathbb{C}_{\mathrm{M}_3^j}, \mathbb{C}_{\mathrm{M}_4^j}$

Computational homogenization

Samples of the meso-scale homogenized elasticity tensors

$\overline{\boldsymbol{\rho}}_{\mathrm{M}^j}$
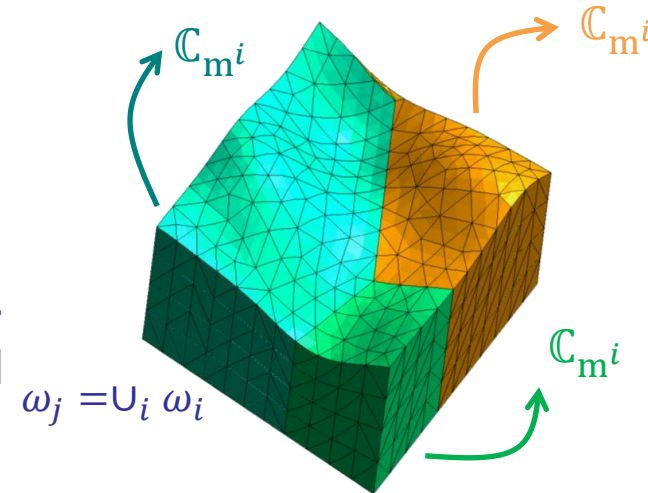
  - The density per unit area is now non-constant

$\boldsymbol{\varepsilon}_{\mathrm{M}}, \boldsymbol{\kappa}_{\mathrm{M}}$

$\widetilde{\boldsymbol{n}}_{\mathrm{M}}, \mathbb{C}_{\mathrm{M}_1}, \mathbb{C}_{\mathrm{M}_2}$

$\widetilde{\boldsymbol{m}}_{\mathrm{M}}, \mathbb{C}_{\mathrm{M}_3}, \mathbb{C}_{\mathrm{M}_4}$

Meso-scale BVP resolution

$\mathscr{A}$

$\overline{h}/2$

$\boldsymbol{\omega} = \cup_i \boldsymbol{\omega}_i$

$\mathbb{C}_{\mathrm{m}^i}$

$\omega_j = \cup_i \omega_i$

Université de Liège

The meso-scale random field

- **Generator of meso-scale random fields**
  - Spectral generator &
  - Non-Gaussian mapping

- **Polysilicon film deposited at 610 ºC**
  - SVE size of 0.5 x 0.5 x 0.5 μm^3
  - Comparison between micro-samples and generated field PDF

$\mathbb{C}_{\mathrm{m}^i}$

$\omega_j = \cup_i \omega_i$

Topology uncertainties effects

- ## Polysilicon film deposited at 610 ºC

  - Cantilever of 8 x 3 x 0.5 μm^3

  - SVE size of 0.5 x 0.5 x 0.5 μm^3

Roughness effect is the most important
for 8 x 3 x 0.5 μm^3 cantilevers
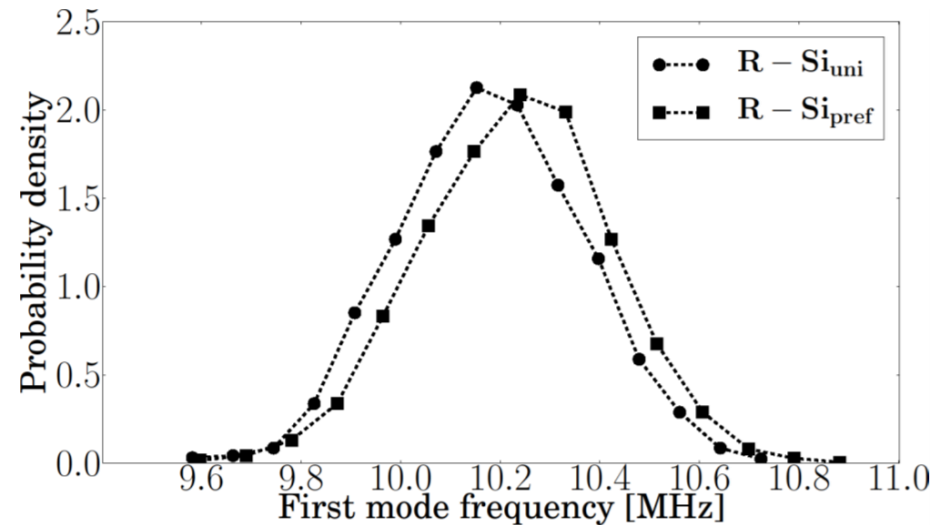
Grain orientation distribution effect
for 8 x 3 x 0.5 μm^3 cantilevers

- Flat SVEs (no roughness) - F
- Rough SVEs (Polysilicon film deposited at 610 ºC) - R
- Grain orientation following XRD measurements – Si_{pref}
- Grain orientation uniformly distributed – Si_{uni}
- Reference isotropic material – Iso

Topology uncertainties effects

- ## Polysilicon film deposited at 610 °C

    - Cantilever of 8 x 3 x 2 μm^3

    - SVE size of 0.5 x 0.5 x 2 μm^3
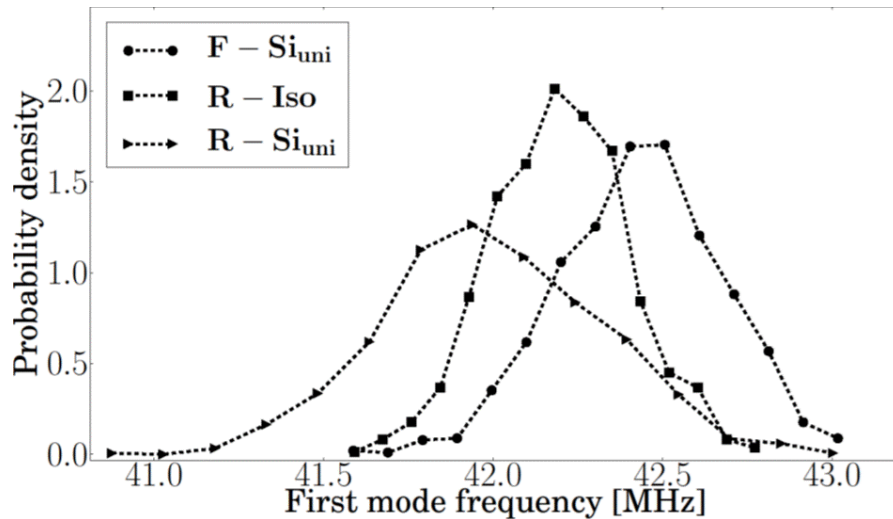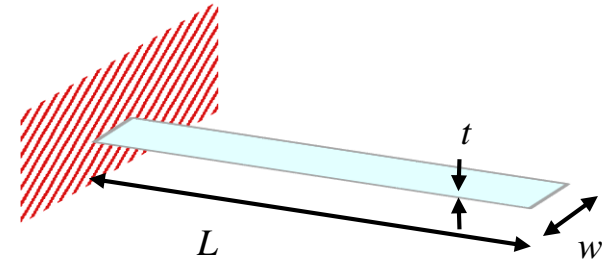
Roughness effect is of same importance as orientation for 8 x 3 x 2 μm^3 cantilevers
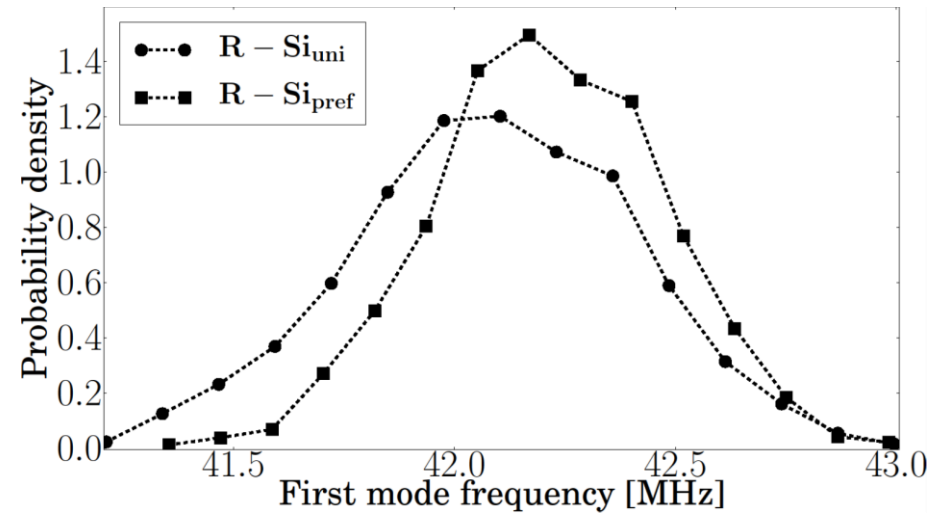
Grain orientation distribution effect for 8 x 3 x 2 μm^3 cantilevers

Conclusions & Perspectives

- Efficient stochastic multi-scale method
  - Micro-structure based on experimental measurements
  - Computational efficiency rely on the meso-scale random field generator
  - Used to study probabilistic behaviors

- Perspectives
  - Other material systems
  - Non-linear behaviors
  - Non-homogenous random fields

Thank you for your attention !

Université
de Liège

Extension to stochastic-plate finite elements

- **Macro-scale Kirchhoff-Love plates**
    - Displacement fields
        - Displacement $\boldsymbol{u}$ of Cosserat plane, and
        - Cross section direction $\boldsymbol{t}$ with
        $$\Delta t_\alpha = -u_{z,\alpha}$$
    - Kinematics: in-plane strain and curvature
    $$\begin{cases} \boldsymbol{\varepsilon}_{M_{\alpha\beta}} = \dfrac{u_{\beta,\alpha} + u_{\alpha,\beta}}{2} \\[2mm] \boldsymbol{\kappa}_{M_{\alpha\beta}} = \dfrac{\Delta t_{\beta,\alpha} + \Delta t_{\alpha,\beta}}{2} = -u_{z,\alpha\beta} \end{cases}$$

    - Resultant in-plane & bending stresses
    $$\begin{cases} \boldsymbol{n}_{M}^{\alpha} = \tilde{n}_{M}^{\alpha\beta} \boldsymbol{E}_\beta = \displaystyle\int_h \boldsymbol{\sigma}_{M}^{\alpha\beta}\, dz\, \boldsymbol{E}_\beta \\[3mm] \tilde{\boldsymbol{m}}_{M}^{\alpha} = \tilde{m}_{M}^{\alpha\beta} \boldsymbol{E}_\beta = \displaystyle\int_h \boldsymbol{\sigma}_{M}^{\alpha\beta} z\, dz\, \boldsymbol{E}_\beta \end{cases}$$

    - Constitutive laws
    $$\begin{cases} \tilde{\boldsymbol{n}}_{M} = \mathbb{C}_{M_1} : \boldsymbol{\varepsilon}_{M} + \mathbb{C}_{M_2} : \boldsymbol{\kappa}_{M} \\[2mm] \tilde{\boldsymbol{m}}_{M} = \mathbb{C}_{M_3} : \boldsymbol{\varepsilon}_{M} + \mathbb{C}_{M_4} : \boldsymbol{\kappa}_{M} \end{cases}$$

$\boldsymbol{u}(x, y) + z\, \Delta t\,(x, y)$

$\boldsymbol{E}_z$ x=cst $\boldsymbol{t}$ y=cst $\mathcal{A}$ y x $\boldsymbol{E}_y$ $\boldsymbol{E}_x$ $\mathcal{S}$

$\boldsymbol{\varepsilon}_M, \boldsymbol{\kappa}_M$ x $\tilde{n}_M, \mathbb{C}_{M_1}, \mathbb{C}_{M_2}$ $\tilde{m}_M, \mathbb{C}_{M_3}, \mathbb{C}_{M_4}$

Meso-scale BVP resolution

$\bar{h}/2$

$\boldsymbol{\omega} = \cup_i \omega_i$
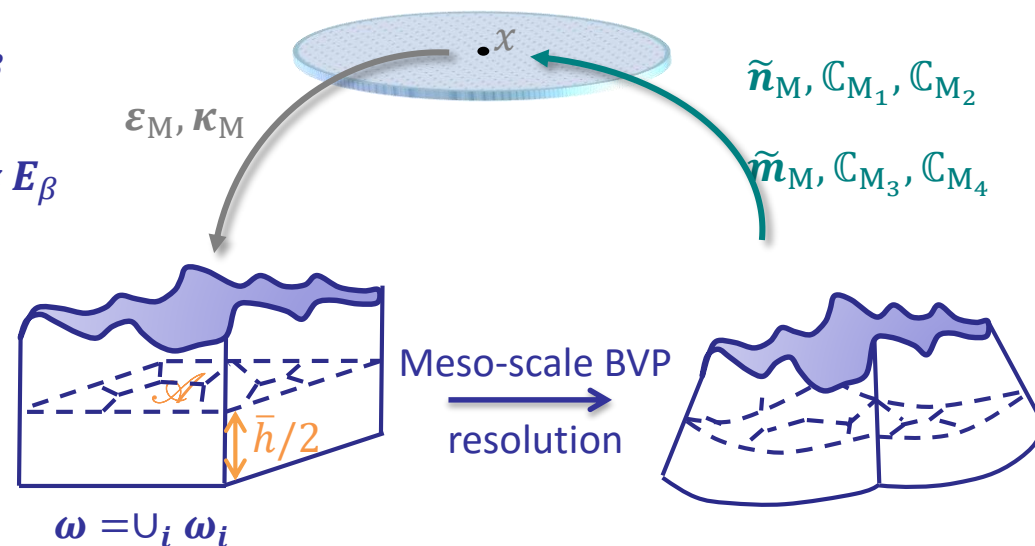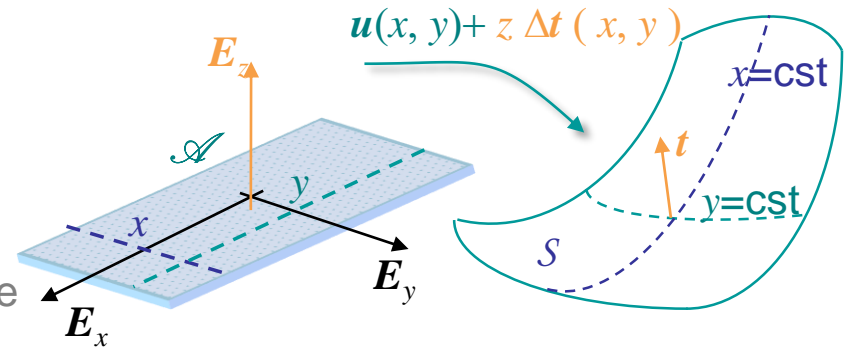
- Stochastic macro-scale Kirchhoff-Love plates
  - Strong form:

$$\begin{cases} \bar{\rho}_{\mathrm{M}}\ddot{u} + (n_{\mathrm{M}}^{\alpha})_{,\alpha} = 0 \\ \\ I_{P_{\mathrm{M}}}\ddot{t} + (-\lambda E_z) + (\widetilde{m}_{\mathrm{M}}^{\alpha})_{,\alpha} = 0 \end{cases}$$

with $\Delta t_{\alpha} = -u_{z,\alpha}$
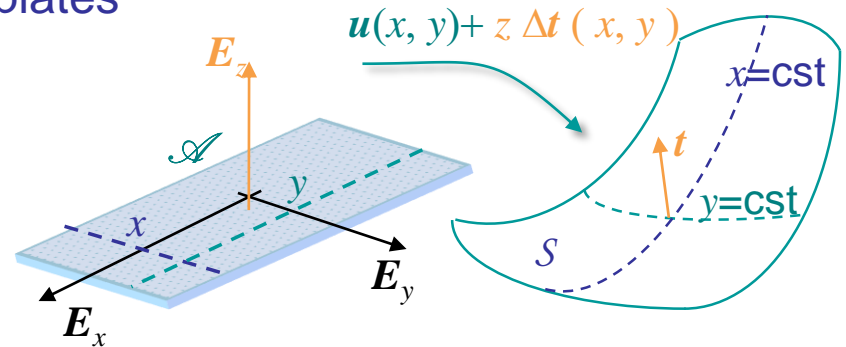
  - Constitutive equations & density per unit area from stochastic homogenization

$$\begin{cases} \widetilde{n}_{\mathrm{M}} = \mathbb{C}_{\mathrm{M}_1}(x, \boldsymbol{\theta}){:}\,\boldsymbol{\varepsilon}_{\mathrm{M}} + \mathbb{C}_{\mathrm{M}_2}(x, \boldsymbol{\theta}){:}\,\boldsymbol{\kappa}_{\mathrm{M}} \\ \\ \widetilde{m}_{\mathrm{M}} = \mathbb{C}_{\mathrm{M}_3}(x, \boldsymbol{\theta}){:}\,\boldsymbol{\varepsilon}_{\mathrm{M}} + \mathbb{C}_{\mathrm{M}_4}(x, \boldsymbol{\theta}){:}\,\boldsymbol{\kappa}_{\mathrm{M}} \\ \\ \bar{\rho}_{\mathrm{M}}(x, \boldsymbol{\theta}) \end{cases} \quad \text{with} \quad \begin{cases} \boldsymbol{\varepsilon}_{\mathrm{M}_{\alpha\beta}} = \dfrac{u_{\beta,\alpha} + u_{\alpha,\beta}}{2} \\ \\ \boldsymbol{\kappa}_{\mathrm{M}_{\alpha\beta}} = \dfrac{\Delta t_{\beta,\alpha} + \Delta t_{\alpha,\beta}}{2} = -u_{z,\alpha\beta} \end{cases}$$

  - Stochastic (Discontinuous Galerkin) finite elements

$$\mathbf{M}(\theta)\ddot{\mathbf{u}} + \mathbf{K}_{uu}(\theta)\mathbf{u} = \mathbf{F}$$

Second-order stochastic homogenization

- **Meso-scale BVP boundary conditions (BCs)**
  - Downscaling

$$
\begin{cases}
\boldsymbol{\varepsilon}_{\mathrm{M}} = \dfrac{1}{V(\omega)} \displaystyle\int_{\omega} \boldsymbol{\varepsilon}_{\mathrm{m}}\, d\omega \\[3mm]
\boldsymbol{\eta}_{\mathrm{M}} \text{ independant of BC}
\end{cases}
$$

$\widetilde{\boldsymbol{n}}_{\mathrm{M}}, \mathbb{C}_{\mathrm{M}_1}, \mathbb{C}_{\mathrm{M}_2}$

$\widetilde{\boldsymbol{m}}_{\mathrm{M}}, \mathbb{C}_{\mathrm{M}_3}, \mathbb{C}_{\mathrm{M}_4}$

$\boldsymbol{\varepsilon}_{\mathrm{M}}, \boldsymbol{\kappa}_{\mathrm{M}}$

Meso-scale BVP resolution

$\boldsymbol{\omega} = \cup_i \boldsymbol{\omega}_i$
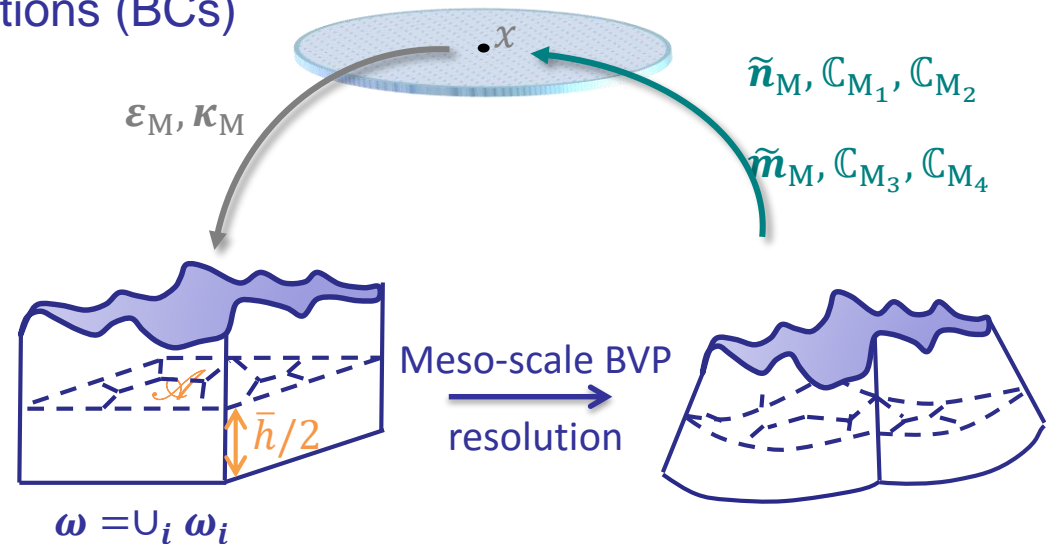
  - Meso-scale BVP fluctuation field

$$
\boldsymbol{u}_{\mathrm{m}} = \boldsymbol{\epsilon}_{\mathrm{M}} \otimes \boldsymbol{x} + \frac{1}{2}\boldsymbol{\eta}_{\mathrm{M}} : (\boldsymbol{x} \otimes \boldsymbol{x}) + \boldsymbol{u}'
\qquad\Longrightarrow\qquad
\begin{cases}
0 = \displaystyle\int_{\partial\omega} \boldsymbol{u}' \otimes \boldsymbol{n}\, d\partial\omega \\[4mm]
0 = \displaystyle\int_{\partial\omega} \boldsymbol{u}' \otimes \boldsymbol{n} \otimes \boldsymbol{x}\, d\partial\omega
\end{cases}
$$

$$
\Longrightarrow
\begin{cases}
\text{Satisfied by periodic and kinematic boundary conditions} \\[2mm]
\text{First equation satisfied by static boundary conditions}
\end{cases}
$$

Université de Liège

Second-order stochastic homogenization

- ## Meso-scale BVP boundary conditions (2)

  - Upscaling

$$
\begin{cases}
\boldsymbol{n}_{\mathrm{M}} = \dfrac{1}{S} \displaystyle\int_{\omega} \boldsymbol{\sigma}_{\mathrm{m}}\, d\omega \\[2em]
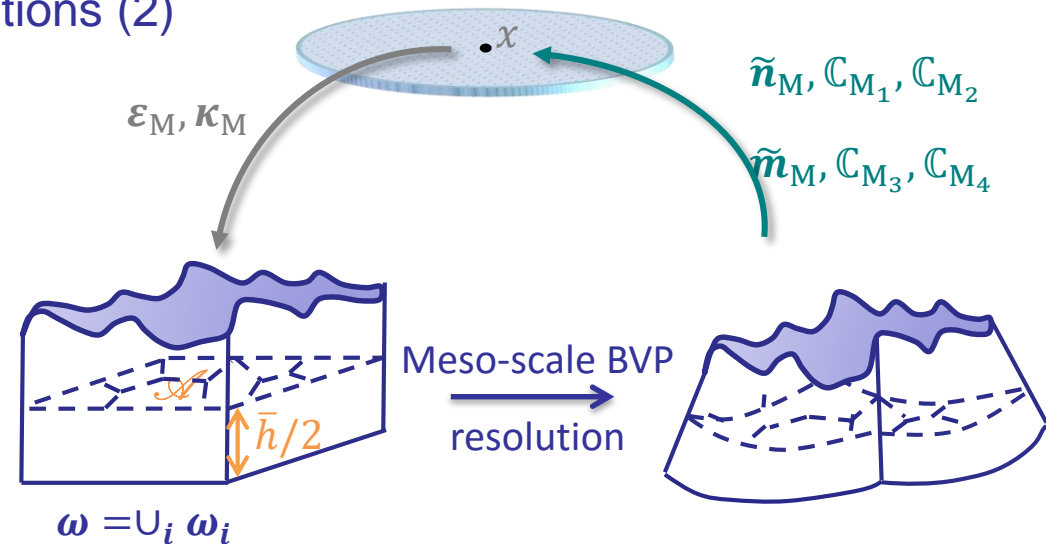\boldsymbol{m}_{\mathrm{M}} = \dfrac{1}{S} \displaystyle\int_{\omega} \boldsymbol{\sigma}_{\mathrm{m}} \otimes \boldsymbol{x}\; d\omega
\end{cases}
$$

$\boldsymbol{\varepsilon}_{\mathrm{M}}, \boldsymbol{\kappa}_{\mathrm{M}}$

$\tilde{\boldsymbol{n}}_{\mathrm{M}}, \mathbb{C}_{\mathrm{M}_1}, \mathbb{C}_{\mathrm{M}_2}$

$\tilde{\boldsymbol{m}}_{\mathrm{M}}, \mathbb{C}_{\mathrm{M}_3}, \mathbb{C}_{\mathrm{M}_4}$

$\mathscr{A}$

$\bar{h}/2$

Meso-scale BVP resolution

$\boldsymbol{\omega} = \cup_i \, \boldsymbol{\omega}_i$

  - Consistency

$$
\boldsymbol{n}_{\mathrm{M}} : \delta\boldsymbol{\varepsilon}_{\mathrm{M}} + \boldsymbol{m}_{\mathrm{M}} : \delta\boldsymbol{\eta}_{\mathrm{M}} = \frac{1}{S}\int_{\omega} \boldsymbol{\sigma}_{\mathrm{m}} : \delta\boldsymbol{\varepsilon}_{\mathrm{m}}\, d\omega \quad\longrightarrow\quad 0 = \int_{\partial\omega} (\boldsymbol{\sigma}_{\mathrm{m}} \cdot \boldsymbol{n}) \cdot \boldsymbol{u}'\; d\partial\omega
$$

⟶ Satisfied by periodic, kinematic, static boundary conditions

  - Top and bottom surfaces
    - Stress free ⟶ plane stress is naturally ensured
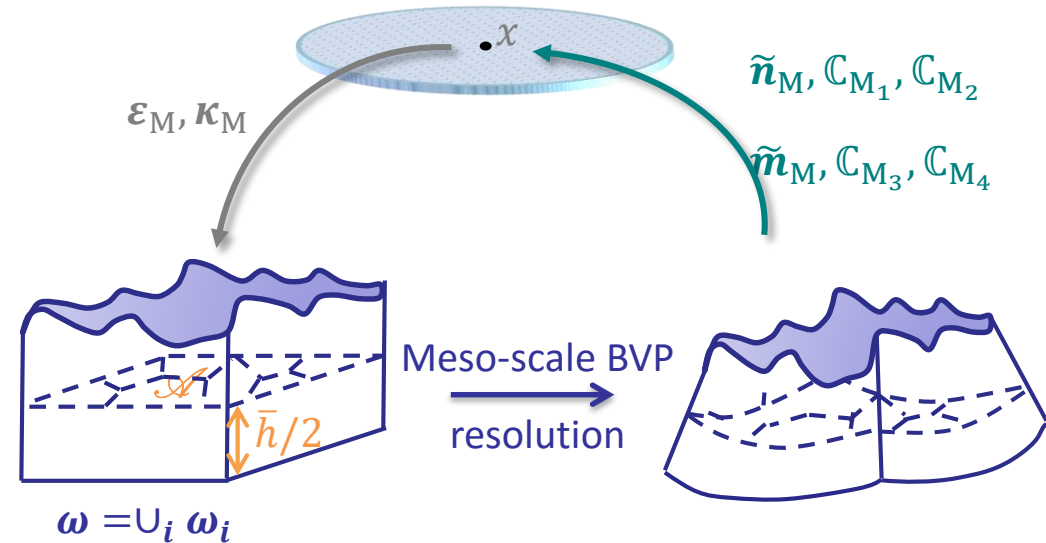 - Side surfaces
    - Mixed boundary conditions

Université de Liège

Second-order stochastic homogenization

- **Second-order homogenization**

  – Downscaling

$$
\begin{cases}
\boldsymbol{\epsilon}_{\mathrm{M}} = \boldsymbol{u}_M \otimes \boldsymbol{\nabla} \\
\qquad = \varepsilon_{\mathrm{M}}^{\alpha\beta} \boldsymbol{E}_\alpha \otimes \boldsymbol{E}_\beta + \hat{\boldsymbol{\epsilon}}_{\mathrm{M}} \\
\\
\boldsymbol{\eta}_{\mathrm{M}} = \boldsymbol{u}_M \otimes \boldsymbol{\nabla} \otimes \boldsymbol{\nabla} \\
\qquad = \kappa_{\mathrm{M}}^{\alpha\beta} \boldsymbol{E}_\alpha \otimes \boldsymbol{E}_\beta \otimes \boldsymbol{E}_z + \hat{\boldsymbol{\eta}}_{\mathrm{M}}
\end{cases}
$$

  - $\hat{\boldsymbol{\epsilon}}_{\mathrm{M}}$ & $\hat{\boldsymbol{\eta}}_{\mathrm{M}}$ undefined for KL plates

  $\boldsymbol{\varepsilon}_{\mathrm{M}}, \boldsymbol{\kappa}_{\mathrm{M}}$ $\tilde{\boldsymbol{n}}_{\mathrm{M}}, \mathbb{C}_{\mathrm{M}_1}, \mathbb{C}_{\mathrm{M}_2}$

  $\tilde{\boldsymbol{m}}_{\mathrm{M}}, \mathbb{C}_{\mathrm{M}_3}, \mathbb{C}_{\mathrm{M}_4}$

  Meso-scale BVP resolution

  $\mathscr{A}$ $\bar{h}/2$

  $\boldsymbol{\omega} = \cup_i \, \boldsymbol{\omega}_i$

  – Upscaling

$$
\begin{cases}
\boldsymbol{n}_{\mathrm{M}} = \dfrac{1}{S} \displaystyle\int_\omega \boldsymbol{\sigma}_{\mathrm{m}} \, d\omega = \tilde{n}_{\mathrm{M}}^{\alpha\beta} \boldsymbol{E}_\beta \otimes \boldsymbol{E}_\beta + \hat{\boldsymbol{n}}_{\mathrm{M}} \\
\\
\boldsymbol{m}_{\mathrm{M}} = \dfrac{1}{S} \displaystyle\int_\omega \boldsymbol{\sigma}_{\mathrm{m}} \otimes \boldsymbol{x} \, d\omega = \tilde{m}_{\mathrm{M}}^{\alpha\beta} \boldsymbol{E}_\beta \otimes \boldsymbol{E}_\beta \otimes \boldsymbol{E}_z + \hat{\boldsymbol{m}}_{\mathrm{M}}
\end{cases}
$$

  - $\hat{\boldsymbol{n}}_{\mathrm{M}} = 0$ & $\hat{\boldsymbol{m}}_{\mathrm{M}} = 0$ for KL plates

  $\quad \longrightarrow \quad \hat{\boldsymbol{\epsilon}}_{\mathrm{M}}$ & $\hat{\boldsymbol{\eta}}_{\mathrm{M}}$ eliminated $\quad \longrightarrow$

$$
\begin{cases}
\tilde{\boldsymbol{n}}_{\mathrm{M}} = \mathbb{C}_{\mathrm{M}_1} : \boldsymbol{\varepsilon}_{\mathrm{M}} + \mathbb{C}_{\mathrm{M}_2} : \boldsymbol{\kappa}_{\mathrm{M}} \\
\\
\tilde{\boldsymbol{m}}_{\mathrm{M}} = \mathbb{C}_{\mathrm{M}_3} : \boldsymbol{\varepsilon}_{\mathrm{M}} + \mathbb{C}_{\mathrm{M}_4} : \boldsymbol{\kappa}_{\mathrm{M}}
\end{cases}
$$